nature protocols

PROTOCOL

https://doi.org/10.1038/s41596-020-0370-0

Check for updates

Engineering DNA nanostructures for siRNA delivery in plants

Huan Zhang[1,5], Honglu Zhang[2,5], Gozde S. Demirer[1], Eduardo González-Grandío[1], Chunhai Fan[3] and Markita P. Landry[1,2,4]✉

Targeted downregulation of select endogenous plant genes is known to confer disease or pest resistance in crops and is routinely accomplished via transgenic modification of plants for constitutive gene silencing. An attractive alternative to the use of transgenics or pesticides in agriculture is the use of a 'green' alternative known as RNAi, which involves the delivery of siRNAs that downregulate endogenous genes to confer resistance. However, siRNA is a molecule that is highly susceptible to enzymatic degradation and is difficult to deliver across the lignin-rich and multi-layered plant cell wall that poses the dominant physical barrier to biomolecule delivery in plants. We have demonstrated that DNA nanostructures can be utilized as a cargo carrier for direct siRNA delivery and gene silencing in mature plants. The size, shape, compactness and stiffness of the DNA nanostructure affect both internalization into plant cells and subsequent gene silencing efficiency. Herein, we provide a detailed protocol that can be readily adopted with standard biology benchtop equipment to generate geometrically optimized DNA nanostructures for transgene-free and force-independent siRNA delivery and gene silencing in mature plants. We further discuss how such DNA nanostructures can be rationally designed to efficiently enter plant cells and deliver cargoes to mature plants, and provide guidance for DNA nanostructure characterization, storage and use. The protocol described herein can be completed in 4 d.

Introduction

RNAi is sequence-specific catalytic inhibition of gene expression at the messenger RNA (mRNA) level, which was first observed in petunia plants in 1990 (ref. [1]), and has since been shown to be present in all eukaryotic organisms[2,3]. RNAi, especially through the post-transcriptional gene silencing (PTGS) pathway, is a powerful tool in plant biotechnology research and practice as it (i) enables high-throughput plant genotype–phenotype mapping, (ii) can be used for rapid discovery of plant biosynthetic pathways for pharmaceutical synthesis and lastly (iii) is a green alternative to chemical pesticides as it can confer crop resistance to insects, bacteria, fungi and diverse plant viruses.

However, current biomolecule delivery tools to plants have certain limitations that prevent RNAi from reaching its full potential in plants. Delivery challenges to plants mostly stem from the rigid and multilayered plant cell wall with a strict size exclusion limit of ~5–20 nm (refs. [4,5]). Therefore, few delivery tools exist that can transfer biomolecules into plant cells, each with considerable drawbacks that either limit the range of transformable species (*Agrobacterium*) or exhibit low transformation efficiencies (biolistics). A common RNAi cargo for plant gene silencing is siRNA, and it is typically delivered to plants via agroinfiltration of viral vectors[6–8]. This method results in strong expression of siRNA, but siRNA needs to be coded as DNA in the viral vector. Additionally, due to the use of pathogenic *Agrobacterium*, this method is useful for a limited range of plant species and has been reported to silence off-target genes in some studies[9,10]. Importantly, the use of *Agrobacterium* for siRNA delivery triggers public and regulatory concern as it creates genetically modified organisms.

Nanomaterials can offer solutions to plant biomolecule delivery challenges given their small size and tunable physical, chemical and mechanical properties. Previously, polymeric nanoparticles have been used to deliver siRNA into tobacco protoplasts, which are plant cells with removed cell walls[11]. This early study demonstrates the potential of nanomaterials in plant systems for RNAi, however, for field applications of RNAi, delivery of siRNA will need to be accomplished in intact plant systems. Another notable study has shown passive delivery of pathogen-specific double-stranded RNA with

[1]Department of Chemical and Biomolecular Engineering, University of California Berkeley, Berkeley, CA, USA. [2]California Institute for Quantitative Biosciences (QB3), University of California Berkeley, Berkeley, CA, USA. [3]School of Chemistry and Chemical Engineering, and Institute of Molecular Medicine, Renji Hospital, School of Medicine, Shanghai Jiao Tong University, Shanghai, China. [4]Chan-Zuckerberg Biohub, San Francisco, CA, USA. [5]These authors contributed equally: Huan Zhang, Honglu Zhang. ✉e-mail: landry@berkeley.edu

clay nanosheets into intact tobacco leaves for insect resistance applications[12], which is a promising use of nanoparticles for topical application of RNAi cargoes on plants. Lastly, a recent study has demonstrated that single-walled carbon nanotubes (SWNTs) can deliver a different RNAi cargo, siRNA, into intact plant leaves without biolistic force, for silencing of transgenes and disease-relevant endogenous plant genes[13].

The emergence of DNA nanotechnology has provided a promising and highly tunable platform with which to design, synthesize and utilize DNA nanostructures to deliver cargoes to mammalian cells[14–19]. Herein, we focus on a recent development demonstrating that DNA nanostructures can also be made to passively bypass the plant cell wall for gene silencing applications. DNA nanotechnology leverages the programmability of DNA Watson–Crick base pairing to assemble nanostructures into custom predesigned shapes, along with precisely tunable mechanical properties. Although a plethora of different DNA nanostructures of variable sizes and shapes have been synthesized and have been utilized in biotechnology for drug, DNA, RNA and protein delivery applications in animal systems[16–21], until our work, DNA nanostructures had not been explored for delivery applications in plant systems despite their utility in other sectors of biotechnology.

In this protocol, we focus on two recent developments in plant bionanotechnology for siRNA-based RNAi applications. First, the unprecedented programmability of nucleic acids can endow DNA nanostructures with prescribed geometrical and mechanical properties[22,23], which can be employed as a potential carrier platform for biological cargoes[21,24]. Second, this advance in DNA nanotechnology has enabled the demonstration that DNA nanostructures can force-independently internalize into intact plant cells of many plant species and deliver siRNA for efficient gene silencing. As not all nanostructure physiochemical parameters are conducive to plant cell internalization, we also determined the optimal nanoparticle parameters for maximum plant cell uptake and gene silencing[25], which enables the rational design of nanoparticles for previously mentioned RNAi applications in plants.

Overview of the procedure

This protocol describes the design and preparation of different DNA nanostructures for delivery of siRNA into mature plants (Steps 1–5). We provide the requisite characterization methods for DNA nanostructure design (by simulating the nanostructure 3D solution geometry and stiffness, and calculating its size and compactness) and validation of correct DNA nanostructure formation through gel electrophoresis and atomic force microscopy (AFM; Step 6). We highlight the checkpoint steps to assess procedural quality (including correct formation of the DNA nanostructures, successful formation of siRNA duplexes and correct siRNA loading onto the DNA nanostructures) before proceeding with downstream gene silencing applications in plants. We next detail how to assess the cellular internalization efficiency of DNA nanostructures following nanostructure infiltration into mature plant leaf tissue of green fluorescent protein (GFP) transgene expressing mGFP5 *Nicotiana benthamiana* (mGFP5 *Nb*). Confocal microscopy and colocalization fraction analysis of the nanostructure with the cytosol of mGFP5 *Nb* are used to evaluate the nanostructure internalization efficiency (Steps 7–11). siRNA can next be loaded onto DNA nanostructures through base-paring hybridization to predefined nanostructure loci, and infiltrated into mature plant cells for gene silencing; the siRNA duplex formation and loading efficiency can be assessed by gel electrophoresis (Steps 12–14). Confocal microscopy, quantitative PCR (qPCR), and western blotting are implemented to evaluate and quantify gene silencing efficiency (Step 15) at the level of (i) fluorescence (via confocal microscopy), (ii) mRNA (via qPCR) and (iii) protein (via western blotting). Throughout the procedure (Fig. 1), we highlight the parameters that can be tuned for optimization or modification, and how to troubleshoot issues possibly encountered during the procedure.

Applications and impact of the method

In this protocol, we utilize recent advances in DNA nanostructure synthesis, demonstrating how to achieve control over DNA nanostructure size, shape, stiffness and compactness[23]. We next leverage the aforementioned developments in nanostructure synthesis to demonstrate that DNA nanostructures can be rationally designed for internalization into mature plant cells and can deliver siRNA to effectively silence a constitutively expressed gene in *Nb* leaves[25]. We discuss how the nanostructure internalization into plant cells and corresponding gene silencing efficiency depend on the nanostructure size, shape, compactness and stiffness, noting that nanoparticle plant cell internalization

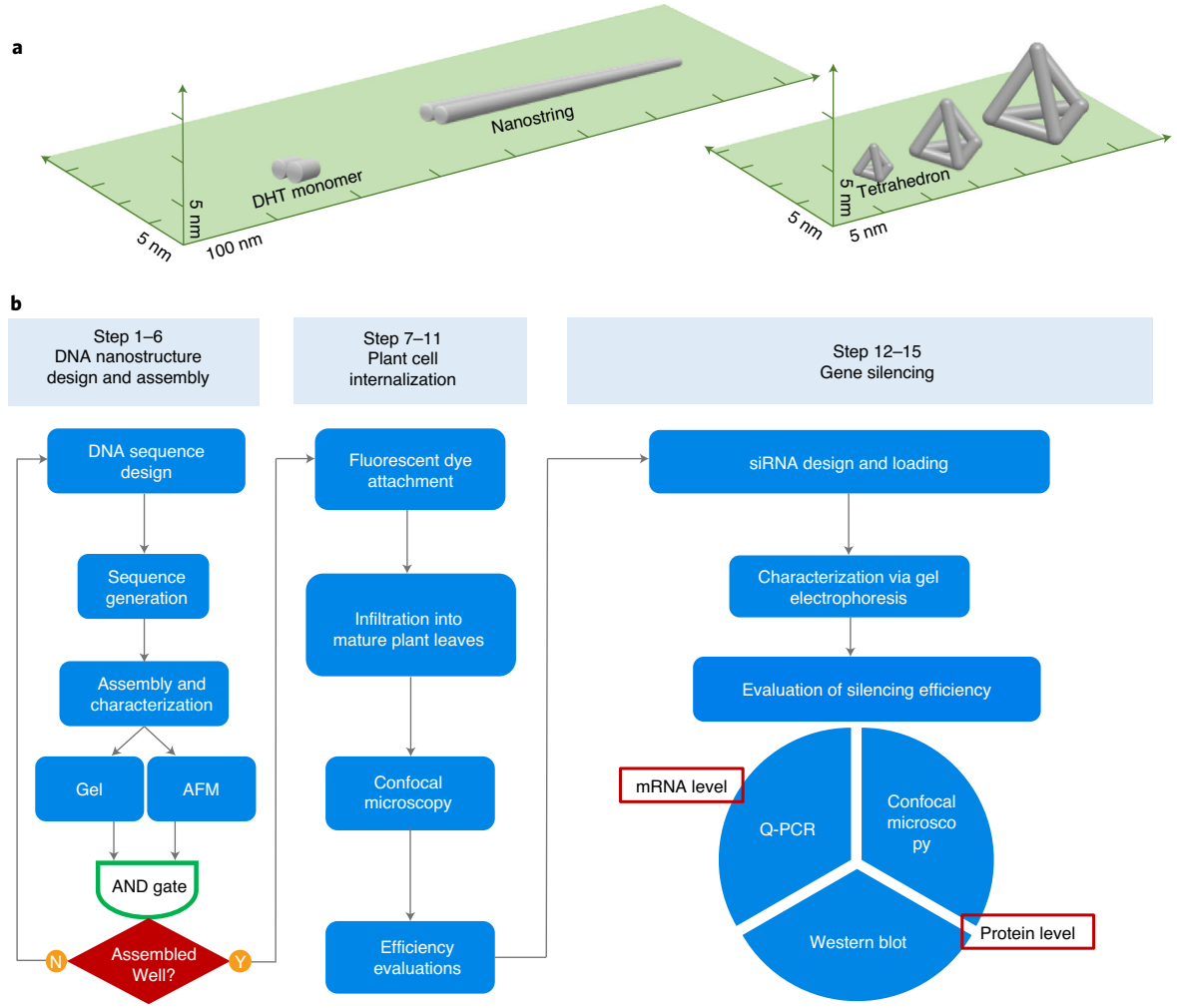

Fig. 1 | DNA nanostructures and workflow for DNA nanostructure design, assembly, characterization and use for siRNA-based gene silencing in plants. a, Schematic illustration of the designed DNA nanostructures. **b**, Workflow and steps of this protocol, where AND gate means both gel and AFM characterization must be used to validate formation of the nanostructure.

mechanisms are vastly understudied, although some analogies may be drawn from prior work done in mammalian cells[26].

Briefly, DNA nanostructures with at least one lateral dimension below ~10 nm and high stiffness show higher cellular internalization into *Nb* tobacco plant cells and correspondingly result in higher gene silencing efficiencies. The strong dependence of cellular uptake on the nanostructure geometry and stiffness provides important clues for enhancing biomolecule delivery to plants following *Nb* nanostructure conjugation to DNA, RNA or protein. In sum, DNA nanostructures can be employed as a programmable toolset for the delivery of exogenous biomolecules such as siRNA to plants. As such, this protocol can be highly useful for plant biologists and crop scientists, and it can be completed within 4 d using only standard benchtop biology laboratory equipment.

The protocol is fundamentally generic for siRNA loading to DNA nanostructures, therefore potential users can substitute their siRNA of interest for their own gene target(s). The generalizability of this platform can enable other applications such as post-translational mediated protein or enzyme modification[27] or in-plant engineering of efficient immune responses[28]. Furthermore, with additional modifications to the constituent building blocks of DNA nanostructures[29], the stability of nanostructures can be improved with incorporation of polymer/protein coatings or backbone modifications, where the versatility of ligand attachment to nanostructures can enable loading of other molecular cargoes of interest such as DNA, guide RNA, peptides or proteins, to realize a variety of targeted delivery and functional assays in plants.

Comparison with other methods

Despite the utility of plant biotechnology, many plant species and tissue types remain difficult to engineer[30] and are subject to species- or tissue-dependent optimizations for genetic engineering procedures. The challenge of delivering genetic cargoes to plant systems is due mainly to the presence of a rigid cell wall that has a relatively small (~20 nm) size exclusion limit[31], which makes it difficult for biomolecules such as DNA, RNA or protein to cross unassisted. Among the aforementioned cargoes, siRNAs are a promising tool that can suppress expression of specific genes by triggering sequence-specific target gene silencing followed by mRNA degradation or translational inhibition[32,33]. To date, several methods have been established to deliver siRNA into plant protoplasts, intact plant cells, or tissues (Table 1). The conventional biotic method of *Agrobacterium*-mediated delivery encodes the RNA into a DNA vector[7,34] and thus suffers from host species limitations that can also result in off-target effects such as random site integration and endogenous gene disruption. Other methods, which employ external forces (for example, high pressure or laser power), such as biolistic delivery and high-pressure spraying may cause variable extents of damage[35,36].

Nanomaterials have emerged as promising carriers for delivery of genetic cargoes to intact plant cells and tissues. Recently, several studies have reported the use of synthetic polymers or peptides to deliver siRNA into protoplasts[11], suspension plant cells[37,38] and tissues[39]. These methods have shown the possibility of nanoparticle internalization into walled plant cells and have thus shown that nanomaterials can serve as carriers to deliver functional siRNA cargoes and achieve various gene silencing efficiencies (Table 1). However, the morphology of such polymer-based carriers is difficult to control and manipulate, and their adaptability for use in mature plants is understudied. Recently, several groups have studied other types of nanomaterials, such as clay nanosheets[12,40] carbon nanotubes[13], and carbon dots[41], to deliver siRNA into intact mature tissues (leaves and roots) for gene silencing, some of which have demonstrated better controllability and increased silencing efficiency compared with polymeric systems.

The DNA nanostructure-based siRNA delivery platform we present herein enables siRNA delivery and gene silencing without transgene integration, with high efficiency, and without toxicity or tissue damage[25]. The DNA nanostructures described herein can enter plant cells without force, and uptake is plant species independent. More importantly, the siRNA targeting sequence and attachment loci can be easily tuned for various gene targeting applications. This technology is easy, fast, cost-effective, nondestructive and scalable. Additionally, DNA nanostructures protect siRNA against nuclease degradation inside plant cells, which indicates the possibility to extend this platform to other biological cargoes of interest.

Limitations

The limitations of this technique include adapting, testing and optimizing nanostructures for use in other plant species and tissues. Variations in nanostructure size, shape, stiffness or compactness may be required to identify maximal nanostructure internalization upon exposure to different plant species and tissues, which may have different morphologies. In such cases, testing several nanostructures with variable structural parameters may first be required, before selecting the nanostructure of choice for subsequent gene silencing applications via siRNA delivery. As shown previously for non-plant systems[18–20,24], with additional nanostructure modification, it may also be possible to attach different cargoes to nanostructures (DNA, RNA and protein) for delivery to plants. For protein loading, optimization of the protein conjugation chemistry would be needed. Additionally, loading of different cargoes may also affect the final properties of nanostructures, in which case systematic testing of several candidate nanostructures may be needed as well. While this protocol demonstrates DNA nanostructure use for gene silencing in mature plant leaves, we recommend that the parameters we discuss—size, shape and stiffness—can be modified to optimize nanostructures for efficient internalization and delivery to other plant samples such as embryonic tissue, germline cells and callus. The aforementioned optimizations might be needed for different plant species or tissue samples that are different in tissue morphology from the plant leaf tissues assayed herein.

Experimental design

To systematically study how the structural and mechanical parameters (size, geometry and stiffness/compactness) of DNA nanostructures impact their internalization into plant cells, a variety of DNA nanostructures with different dimensions and geometries are designed (Supplementary Discussion

Table 1 | Summary and comparison of the siRNA delivery methods in plants

Delivery platform			Target species/ tissue	Target gene	Mechanical parameter	Silencing efficiency	siRNA loading strategy	Limitation/advantage
Biological-assisted delivery		*Agrobacterium*-mediated virus-induced delivery[7,34,54]	Mature plants/intact tissues	Phytoene desaturase (PDS) genes; GFP; AG, CLV3, AP1 and PAN	—	High	Encode into DNA vector	Host species limited; need extra encoding process
Physical-assisted delivery		Biolistic delivery (particle bombardment)[55,56]	Single epidermal cells; mature tissue (leaves)	C1 plus B-Peru genes; GFP;	—	2 μg siRNA per shot for strong RNAi	Adsorption-based coating, then shooting	Possible physical damage to plant tissue and detach of siRNA
		High-pressure spraying[35]	Mature tissue (leaves); apical buds	GFP	—	Local and systemic RNA silencing.	No loading	Less potential physical damage to plant tissue, no damage to siRNAs.
		Nanosecond pulsed laser-induced stress wave (LISW)[36]	Suspension cells	GFP	—	3 μg of siRNA, 80–95% efficiency (protein level)	No loading	Need professional and expensive equipment
Chemical-assisted delivery	Polymer/peptide-mediated delivery	Conjugated polymer nanoparticles (CPNs)[11]	BY-2 protoplasts	NtCesA-1, (cell wall synthesis)	Hydrodynamic radius 60–80 nm; positively charged	200 nM siRNAs, 51–54% efficiency	Electrostatic absorption	Non-toxic, only validated in protoplasts
		Polyethyleneimine (PEI)[37]	Transgenic rice cells	T-lymphocyte antigen 4-immunoglobulin (hCTLA4Ig)	Micrometer (μm); PEI, PVA, PVP, 8 and 20 kDa PEGs positively charged	3 μg siRNA; 70.6% efficiency	Electrostatic absorption	Only validated in suspension cells; potential toxicity
		Cationic oligopeptide polyarginine (POA)[38]	Tobacco (*Nicotiana tabacum*) suspension cells	GUS NPTII	12 arginines positive charged	10 μg (NPTII) or 20 μg (GUS) dsRNA; completely degraded corresponding mRNA after certain time (24 or 72 h)	Electrostatic absorption	Only validated in suspension cells
		Peptide[39]	Mature tissue (leaves)	Yellow fluorescent protein (YFP); chalcone synthase (CHS)	100–300 nm in diameter; positively charged	20 pmol dsRNA; 70% efficiency for YFP	Electrostatic absorption	Quick and local gene silencing
	Nanoparticle-mediated passive delivery	Layered double hydroxide (LDH) nanosheets[12,40]	Mature tissue (roots, leaves), BY-2 cells	Pepper mild mottle virus (PMMoV) and cucumber mosaic virus (CMV)	15–120 nm with an average diameter of 45 nm, lateral dimension in the range of 20–80 nm; positively charged	Significant downregulation	Electrostatic absorption	Sustained release of cargo; unknown target species range
		Carbon dots[41]	Mature tissue (leaves)	GFP; magnesium chelatase (MgChe)	Hydrodynamic radius range from 1 to 30 nm depending on the molecular weight of PEI ligand	12 ng/μL siRNA 84% efficiency for GFP; 79% efficiency for MgChe	Electrostatic absorption	Silencing can be achieved with relatively low amounts of siRNA. Need PEI modification during the synthesis, introducing potential toxicity
		SWNTs[57,58]	Mature tissue (leaves)	GFP	1 nm in diameter with an average length of 500 nm	100 nM siRNAs; 95 ± 4.1% for a siRNA, 92 ± 6.2% for b siRNA (mRNA level); 42.6 ± 2.8% (protein level)	Non-covalently adsorption via π–π stacking	Specific and transient gene targeting; protection of siRNA from nuclease degradation
		DNA nanostructures	Mature tissue (leaves)	GFP	Tetrahedron: 2.4 nm; HT monomer: (2 × 5 × 16 nm); nanostring: (2 × 5 × 320 nm)	100 nM siRNAs; 40–59% (varies with DNA structures) in both mRNA and protein level	Nucleotide base pairing hybridization	Specific and transient gene targeting through sequence design; controllable attachment; protection of siRNA cargo; no toxicity or damage

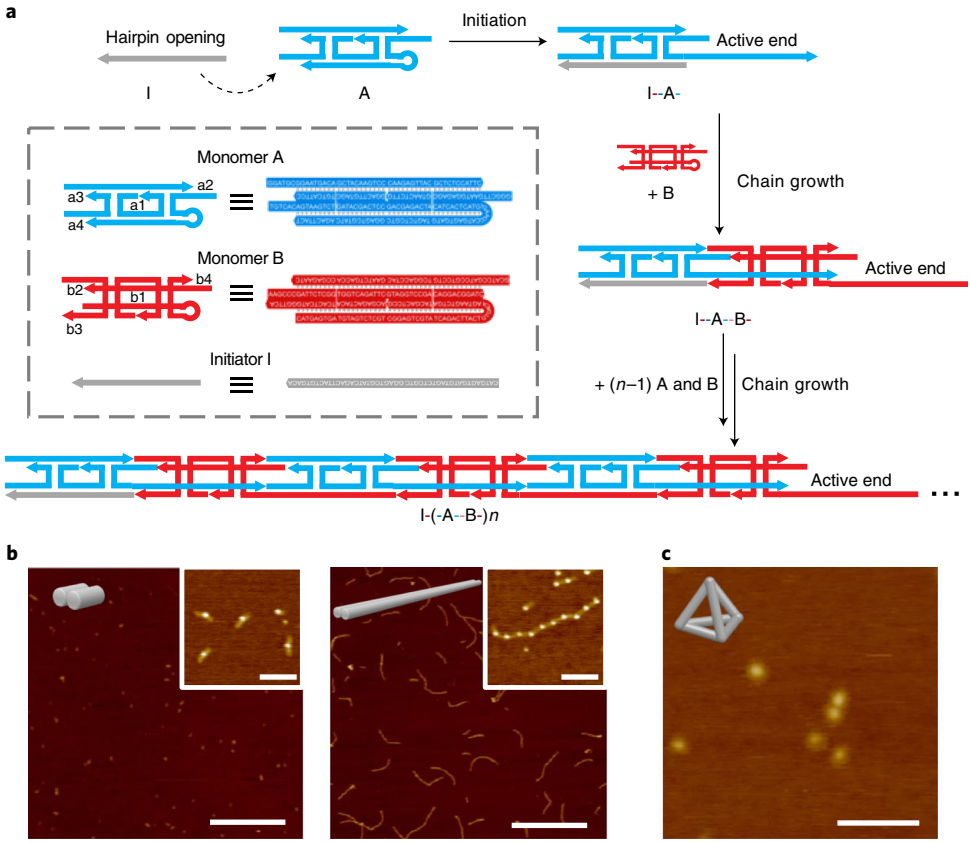

Fig. 2 | Assembly and characterization of DNA nanostructures. a, Chain-growth co-polymerization of nanostring from DHT monomers A and B, initiated with I. The DHT copolymerization starts only with an initiator I to activate a metastable monomer A. The exposed sequence of A invades and thus activates the hairpin domain of B with an exposed sequence (identical to I), which can then further activate another monomer A. The exhaustion of monomers terminates the nanostring polymerization, whereas the preformed nanostring retains active sites such that the addition of new monomers can resume the reaction, if the user wishes to further elongate the nanostring. **b**, Representative AFM images of DHT monomers (left) and nanostring (right) (insets: biotin–streptavidin-labeled DHT monomers and nanostring). Scale bar: 500 nm. (inset scale bar: 100 nm). **c**, Representative AFM images of tetrahedron. Scale bar: 100 nm.

and Supplementary Tables 1 and 2). Specifically, here we outline how to design DNA hairpin tiles (DHTs), DNA nanostrings and DNA tetrahedra.

DNA nanostructure design and assembly

DNA hairpin tiles. DHT is a novel genre of 'double-crossover' (DX) tile, which comprises two Holliday junctions (crossovers) between two double helices. The conventional DX tile[42] is fixed and is used for assembling into unbounded arrays. In comparison, the DHT possesses potential energy by virtue of its metastable hairpin, which can be initiated into an active form to enable self-assembly of multiple nanostructure tiles into linear arrays. Accordingly, the size and length of DNA nanostrings can be precisely controlled by the regulation of DHT chain growth. Two monomers of DHT, A and B (Fig. 2a), are designed to be assembled with four sequences, separately. Each DHT is ~2 × 5 × 16 nm in size and comprises three functional domains: a static DX core (strand a1 or b1 in Fig. 2a), in which a pair of crossover junctions stabilize the two double helices, and two corner sticky ends of single strands (5′ ends of a2, a4, b2 and b3 in Fig. 2a), which associate with the corresponding domains of neighboring monomers. The 5′ sticky end of strand a2 hybridizes to the 5′ end of b2, and the 5′ end of a4 is complementary to the 5′ end of b3 (Fig. 2a).

Importantly, each DHT monomer is designed with the addition of a hairpin domain (a4 and b4 in Fig. 2a) with the toehold sequence, which enables self-assembly of DHT monomers into DNA nanostrings as detailed in the following section. These DHT monomers can be subsequently characterized as detailed below in Step 6, before use for internalization and gene silencing assays in plants.

DNA nanostring. With the incorporation of metastable hairpins, DHTs can be activated by an initiator strand (I), which is designed to match the hairpin stem sequence of monomer A (Fig. 2a). The initiator induces a conformational change in the DHTs and triggers a cascading strand displacement reaction[43] during chain-growth copolymerization, enabling the generation of polymeric assemblies of DHTs into nanostrings. In principle, chain-growth copolymerization (Fig. 2a) is activated via the invasion of initiator I to monomer A, producing a complex I–A with a reactive terminus, whereby DHT-based chain growth only occurs with introduction of the initiator. Monomer B is designed to react with the I–A terminus and is activated to produce a complex I–A–B with a new reactive terminus, which invades the next monomer A. Subsequently, this chain grows with sequential addition of monomers to these active termini, thus chain-growth copolymerization happens via this initiation and propagation processes. At ambient temperature conditions, the metastable hairpin structure is stable because the topological constraint of the loop domains of DHTs blocks the reaction of neighboring monomers in the absence of initiators. Copolymerization is triggered exclusively with the introduction of initiator strand I, which invades the toehold sequence and subsequently opens the hairpin domain of monomer A. The activated monomer A exposes its loop terminus to react with the toehold for further activation of monomer B, whose exposed terminus would react with another monomer A. Simultaneously, the interactive associations of the corner sticky ends of neighboring monomers also facilitate and stabilize the copolymer chains in close proximity. Consequently, once the initiator I triggers the reaction with A, the subsequent chain grows in a self-propagating manner to copolymerize into a one-dimensional nanostring structure. Specifically, assembly of the 10-mer nanostrings used here is carried out in an aqueous solution containing 1 μM equivalents of monomers A and B and 0.1 μM initiator I (molar ratio = 10:1). The DNA mixture is further incubated at room temperature (RT; 20 °C) for 1 h to allow nanostring polymeric synthesis.

DNA tetrahedron. Three DNA tetrahedrons with distinct diameters can be designed as in previous studies[44]. Here, four DNA strands are leveraged to assemble into a rigid framework of the DNA tetrahedron. In accordance with the structure of B-form double-helix DNA (2 nm in diameter and 0.33 nm per base in the direction of the helical axis), the dimensions of the tetrahedra will range from 2.4 nm, 8.8 nm to 12.6 nm in edge lengths.

Assembly of DHT monomer, nanostring and tetrahedron. DHT monomer, tetrahedron and nanostring are assembled via a thermal annealing process. To construct each DNA nanostructure, corresponding DNA components as listed below are annealed at high temperature by heating, followed by incremental cooling in 1× Tris-magnesium (TM) or 1× Tris acetate EDTA magnesium (TAEM) buffer. For DHT monomers, stoichiometrically equivalent quantities of four sequences are mixed together with concentrations as specified below, and then annealed in an insulated water bath by first heating the sample to 95 °C, next turning off the water bath and allowing the sample to reach 25 °C over the course of 20 h (ref. [42]). To form the tetrahedron with different sizes, stoichiometrically equivalent quantities of four or eight sequences (Supplementary Table 1) are annealed together as described above by heating to 95 °C, then transferring to an ice bath to allow cooling to 4 °C within 10 min. Assembly of the DNA nanostring is accomplished via higher-order organization of preformed DHT monomers with an isothermal polymerization process. Due to the chain-growth nature of DHT copolymerization, the assembly of nanostrings can be performed at a constant temperature. However, the initiation and propagation of copolymerization require conformational changes of stem-loop structures, so it is necessary to determine the optimal isothermal conditions at which this reaction can take place, which will depend on the stem-loop sequences. In this protocol, we describe the copolymerization of DHT monomers at different constant temperatures (ranging from 46 °C to 25 °C in increments of 3 °C) and variable incubation times (ranging from 24 h, 12 h, 6 h, 3 h, 1 h to 30 min). The optimal isothermal conditions for nanostring assembly were found to be 37 °C for 3 h, however, incubation at 25 °C for 1 h can generate nanostring products with comparable efficiency and size uniformity. The length and size uniformity of DNA nanostrings are governed by the nature of chain-growth polymerization, which provides an efficient approach to achieve regulation over macromolecular organization. For DHT assembly, in which copolymerization is triggered only upon reaction with an initiator to activate a metastable monomer, the chain continuously grows with the association of new monomers. The exhaustion of monomers terminates the polymerization, whereas the preformed nanostring retains active sites such that the addition of new monomers can resume the reaction if the user wishes to elongate the nanostring. To gain control over the final nanostring length, new monomers can be added to the preformed copolymer solution, and the products from each step of monomer addition can be iteratively characterized using AFM until the desired final nanostring

length is achieved (here, ten monomeric units or 320 nm). DNA sequences from which DHT monomers, tetrahedrons and nanostring are synthesized are listed in Supplementary Table 1.

Characterizations of DNA nanostructures

Gel electrophoresis. Following annealing, the DHT monomers and tetrahedrons can be characterized by native PAGE analysis (see images in Supplementary Fig. 1), and the nanostring can be characterized by agarose gel electrophoresis.

AFM imaging. The products of DNA assembly, including DHT monomers, nanostrings and tetrahedrons, can be directly visualized by AFM. Additionally, to confirm (i) the attachment locus onto which siRNA will be attached or (ii) the precise number of DHT monomers that copolymerized onto nanostrings, biotin–streptavidin (bio–STV) interactions can be leveraged to provide a structural label for high-contrast AFM imaging. To confirm correct placement of siRNA attachment loci, a biotin-modified DNA strand can be designed into the tetrahedron or DHT monomer at the position along the nanostructure where one wishes to subsequently attach siRNA. Similarly, to assess nanostring length and proper DHT monomeric composition, a biotin-modified DNA strand can be designed into the construction of each monomer. Nanostructures can then be thermodynamically assembled as described above, for which there will be an accessible biotin to bind streptavidin protein. After assembly of nanostructures, biotinylated nanostructures can be incubated with 5 nM streptavidin for 10 min at 37 °C before AFM imaging. Through AFM imaging, discrete patterns of anchored STVs will allow direct visualization of nanostructure products in which the siRNA attachment locus or number of DHT monomeric subunits in each nanostring can be determined with high accuracy (see representative images in Fig. 2b insert).

Plant growth

Plants should be cultivated using optimal conditions for the particular species being used for experimentation. For the examples shown in this protocol, transgenic mGFP5 *Nb* (from the Staskawicz Lab, University of California, Berkeley—used herein for internalization and gene silencing studies), tobacco, arugula and watercress (used herein for internalization studies) seeds were germinated and kept in SunGro Sunshine LC1 Grower soil mixture within the growth chamber (740 FHLED). The plants were grown at 25 °C, 60% humidity, with an 8-h light cycle per 24 h, and were watered twice a week. Plants 3–4 weeks of age were chosen for experimental use, and infiltrations were performed by gently infiltrating nanostructures with a 1-ml needleless syringe (Step 8, Supplementary Fig. 2) and without using any surfactant.

Nanostructure internalization and silencing efficiency evaluations and controls

To assess nanostructure internalization, we use a Cy3-labeled single-stranded DNA to assemble the nanostructure itself, instead of tagging a preformed DNA nanostructure with a Cy3 overhang. This approach ensures that the final concentration of Cy3 dye and the total amount of DNA are the same for all nanostructures, thus we can evaluate nanostructure internalization based on Cy3 fluorescence that colocalizes with the cytosol, and assess nanostructure internalization efficiency based on nanostructure properties. To assess silencing efficiency, we employ several methods to quantify both the change in mRNA (qPCR) and the protein change (confocal microscopy and western blotting). For qPCR, EF1 (elongation factor 1) was chosen as our housekeeping (reference) gene, which has been shown to be a stable internal control for gene expression as its expression does not fluctuate under a range of treatments[45]. Meanwhile, leaves infiltrated with just buffer (control), siRNA only or DNA nanostructures only are also listed as further control groups to verify that the silencing was caused by the siRNA delivered by the DNA nanostructures, and not by the DNA nanostructures themselves. For confocal microscopy, non-treated *Nb* leaves serve as controls, for which the GFP fluorescence intensity is defined as 1 in the subsequent statistical analyses to determine the silencing efficiency for experimental groups, which are normalized to 1. For western blotting assays to determine GFP protein expression, non-treated *Nb* leaves serve as controls, for which the band intensity is defined as 1 in the subsequent statistical analyses.

Internalization study of DNA nanostructures

To identify which nanostructures internalize into plant cells most effectively, DNA nanostructures with different sizes, shapes and stiffnesses are labeled with Cy3 fluorophores via labeling of the DNA strand used to form the nanostructure, and infiltrated into transgenic mGFP5 *Nb* plants at a concentration of 400 nM. Transgenic mGFP5 *Nb* plants have been engineered to constitutively express

GFP proteins (see GFP expression confirmation in Supplementary Fig. 3). Because GFP localizes in the cytosol, its expression is therefore used as a fluorescent marker for the cell cytosol to calculate colocalization efficiencies in nanostructure internalization studies, and separately serves as the transgene target for siRNA-based gene silencing studies as detailed below. In this manner, for internalization and silencing quantification, colocalization analysis of Cy3-tagged nanostructures with the GFP-labeled cytosol provides a relative measure of nanostructure internalization, and a decrease in GFP fluorescence and expression provides a measure of siRNA-based gene silencing efficiency. In this protocol, plant cell internalization of DNA nanostructures with different sizes, shapes and stiffness/compactness (see details in Supplementary Table 2) are investigated, and their siRNA-based silencing efficiencies are compared. Together with simulation and calculation of DNA nanostructure mechanical parameters based on Cando software[46–48], we find that smaller-sized nanostructures with higher stiffness/compactness can enter the plant cell more efficiently and can silence genes more effectively. Moreover, we show in Supplementary Fig. 4 that DNA nanostructures can enter different plant species (tobacco, arugula and watercress). As such, our study provides guidance on the parameters of importance for designing DNA nanostructures as biomolecule delivery tools for plants, and this protocol can be repeated to test optimal plant cell internalization in different plant species or tissue types. We also investigated the mechanism of DNA nanostructure internalization into plant cells. Results summarized in Supplementary Fig. 5 show a noticeable decrease in DHT monomer internalization when incubated at 4 °C post-infiltration, or if the leaf is pretreated with 33 μM wortmannin[49], a chemical inhibitor of endocytosis, relative to leaves infiltrated with the DHT monomer in the absence of cold or wortmannin. Both of these assays suggest that nanostructure internalization occurs predominantly through an active endocytosis pathway.

Cargo attachment of DNA nanostructures

Each DNA nanostructure can be designed to attach biological or non-biological cargoes, for example, DNA, RNA or fluorescent dyes, to the predefined loci. A DHT monomer as described above contains one attachment locus at either its center (DHT-c) or side (DHT-s). Multiple DHT-c monomers are assembled into one nanostring with corresponding cargo attachment loci. The tetrahedron has one attachment locus at one of its apexes.

Gene silencing efficiency of DNA nanostructures

Tetrahedron, DHT monomer and nanostring nanostructures can be loaded with siRNA via hybridization of single-stranded sRNA complementary to the nanostructure locus or loci, as described above, and infiltrated into transgenic mGFP5 *Nb* plants at an siRNA concentration of 100 nM. A 21-bp siRNA sequence that inhibits GFP expression in a variety of monocot and dicot plants[50] was designed, and this duplex siRNA oligonucleotide was hybridized to a complementary strand programmed into the site-specific loci on the DNA nanostructures (Fig. 3; see Supplementary Table 1 for sequences). Next, infiltration of siRNA-loaded nanostructures into mGFP5 *Nb* is performed, and gene silencing efficiency is assessed 1 or 3 d later through three orthogonal methods: qPCR is performed to check the GFP mRNA level after 1 d, where the change in GFP mRNA levels will reflect variations in GFP expression, confocal microscopy (after 3 d) is performed to directly image and compare GFP fluorescence intensity change, and western blotting (after 3 d) is utilized to further quantify GFP expression changes in the infiltrated leaf tissues by directly quantifying the amount of GFP extracted from treated leaves. With these three methods of evaluating gene silencing, we can design and load different kinds of siRNA to target various genes and compare silencing efficiencies when delivered with different DNA nanostructures. We can also explore the endogenous silencing pathways by which siRNA-loaded nanostructures accomplish gene silencing in plants.

Materials

Biological materials

- In the example described in this protocol, we use transgenic mGFP5 *Nb* plants (seeds obtained from the Staskawicz lab at UC Berkeley).

Reagents

! CAUTION All of the reagents and solvents used in the protocol require the use of protective goggles, gloves and lab coats. All reagents should be stored and prepared according to the manufacturer's

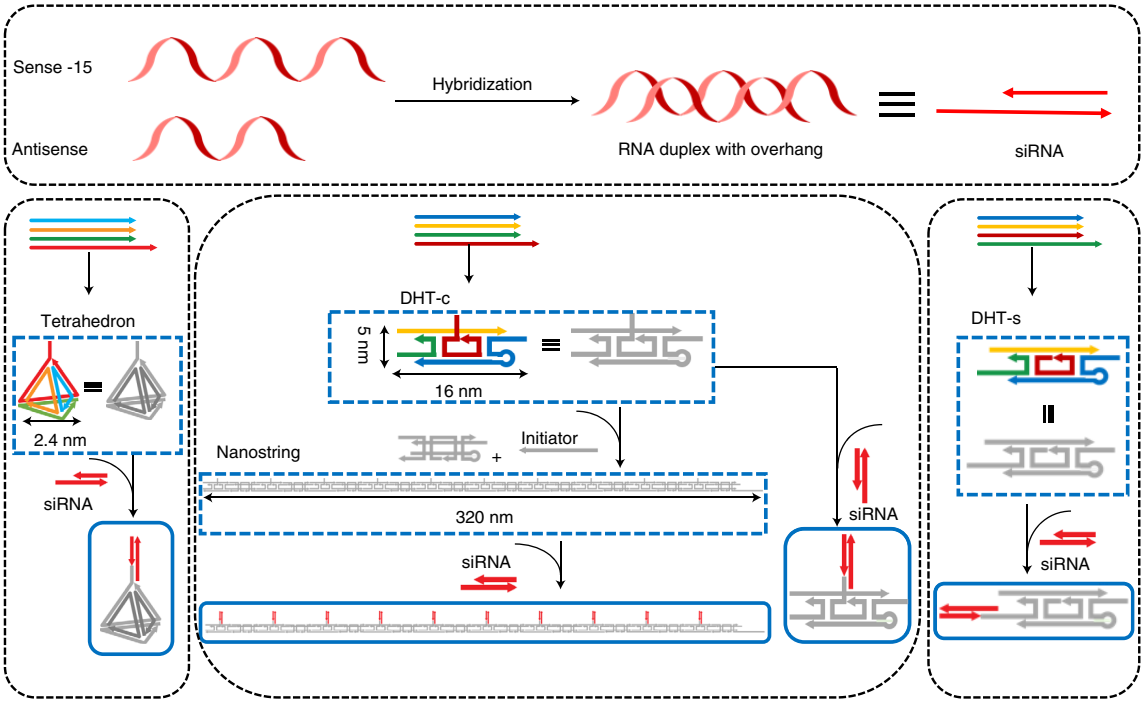

Fig. 3 | Illustration of the design and loading of siRNA duplexes on DNA nanostructures. siRNA duplexes with 15-nt overhangs are formed by hybridization of two complementary single-stranded RNAs. Each nanostructure has a 15-nt overhang at a specific location that is fully complementary to the overhangs on the siRNA duplex (red). The DHT monomer has two potential attachment loci, one at its center (DHT-c) and another at its side (DHT-s). DNA strands forming the tetrahedron and DHT monomer structures are in red, orange, green and blue.

instructions ▲ **CRITICAL** It is strongly recommended that solid and liquid waste generated during this protocol should be disposed of properly, according to local or institutional regulations.

- Anti-GFP antibody, ChIP Grade (Abcam, cat. no. ab290; RRID: AB_303395)
- Goat anti-rabbit IgG H&L (HRP; Abcam, cat. no. ab205718; RRID: AB_2819160)
- Milli-Q water
- Nuclease-free water (Qiagen, cat. no. 129114)
- Single-stranded RNA and DNA oligonucleotides (Integrated DNA Technologies); DNA oligonucleotides labeled with Cy3 are purified by HPLC, see Supplementary Table 1 for the detailed sequences used in this protocol **! CAUTION** Store at −20 °C before and after dissolution to prevent potential degradation with a maximum storage time of 1 year.
- 10× PBS (Corning, cat. no. 46-013-CM)
- Hydrochloric acid (HCl, 37% (vol/vol); Sigma, cat. no. 320331) **! CAUTION** HCl is caustic and can cause harm. Wear proper personal protective equipment (PPE, lab coat, gloves and goggles), and work in a fume hood when handling this reagent.
- Acetic acid (CH_3COOH, 500 ml; Sigma, cat. no. 695092) **! CAUTION** CH_3COOH may cause skin, eye, and respiratory irritation. Wear a lab coat, gloves and safety goggles, and work in a fume hood when handling this reagent.
- Magnesium chloride hexahydrate ($MgCl_2{\cdot}6H_2O$; Sigma, cat. no. M2670) **! CAUTION** This reagent may cause irritation to the eyes and skin.
- Magnesium acetate tetrahydrate ($MgAc_2{\cdot}4H_2O$; Sigma, cat. no. M5661-250G)
- Tris base (Fisher scientific, cat. no. BP152-500g)
- Sodium chloride (NaCl; Sigma, cat. no. S7653-1KG)
- EDTA (RPI, cat. no. E57040-100)
- Tergitol NP-40 nonionic surfactant (Pfaltz and Bauer, cat. no. T01164-500g)
- Glycerol (Fisher Scientific, cat. no. G33-500)
- Ammonium persulfate (APS; Sigma, cat. no. 248614-100G)
- Low range ultra agarose (Bio-rad, cat. no.1613107)
- Tween 20 (Sigma, cat. no. P1379-100ML)
- *N,N,N′*-Tetramethylethylenediamine (TEMED; Sigma, cat. no. T9281)

- Glycine (Sigma, cat. no. G8898)
- PVDF membrane, precut, 7 × 8.4 cm (Bio-rad, cat. no. 1620174)
- Methanol (Sigma, cat. no. 179957)
- 4× Laemmli sample buffer (10 ml, Bio-rad, cat. no. 1610747)
- Liquid nitrogen **! CAUTION** Liquid nitrogen can cause burns. Wear cryo gloves to protect hands and safety goggles or a face shield to protect eyes when handling this reagent. Always wear appropriate PPE (lab coat, closed-toe shoes and long pants).
- SYBR Gold nucleic acid gel stain (Invitrogen, no. S11494)
- 30% (wt/vol) acrylamide/bis solution 19:1 (Bio-rad, cat. no. 1610154)
- Pierce 660 nm protein assay (Thermo, product no. 22660)
- iScript cDNA synthesis kit (Bio-Rad, cat. no. 1708891)
- PowerUp SYBR green master mix (Applied Biosystems, cat. no. A25742)
- RNeasy plant mini kit (Qiagen, cat. no. 74904)
- Protease inhibitor cocktail (Sigma, cat. no. P9599-1ML)
- Amersham ECL prime western blotting detection reagent kit (GE Healthcare, cat. no. RPN2232)

Equipment

- Conical tubes (50 ml; Olympus, cat. no. 28-106)
- Pipette tips (Low retention 10 µl, 200 µl, 1,000 µl filter tips; USA Scientific, cat. nos 1181-3710, 1180-8710, 1182-1730)
- Syringe (1 ml; BD, cat. no. 14-823-434)
- Sterile syringe filter (0.45 µm; VWR, cat. no. 28145-481)
- Microcentrifuge tubes (1.5 ml; VWR, cat. no. 89000-028)
- Analytical balance (Radwag, AS 60/220.R2)
- Scissors (VWR, cat. no. 82027-582)
- Mortar and pestle (Cole-Parmer, cat. no. EW-63100-54)
- Microscopy cover glass (Fisher Scientific, cat. no. 12-542B)
- Microscope slides (VWR, cat. no. 16004-422)
- Centrifuge (Eppendorf, cat. no. 5424R)
- Vortex mixer (Fisher Scientific, cat. no. 02-215-365)
- Orbital shaker (Waverly, cat. no. S1CE)
- UV-3600 Plus UV–Vis NIR spectrophotometer (Shimadzu Scientific Instruments, Columbia, MD)
- pH meter (Spectrum, cat. no. 242-97839)
- EasyStrip Plus PCR tube (Thermo Scientific, cat. no. AB2005)
- Gel image-analysis system (Typhoon FLA 9500, GE Healthcare Services)
- Mica sheet, 1 × 3 inches (Ted Pella, cat. no. 53)
- AFM (MultiMode 8, Bruker)
- AFM tip (TESP-SS, Bruker)
- Confocal microscope (Zeiss LSM 710)
- Thermal Cycler PCR (Applied Biosystems Veriti 96-Well, cat. no. 4375786)
- Thermal Cycler CFX96 Touch real-time PCR detection system (Bio-rad, cat. no. 1855195)
- NanoDrop One microvolume UV–Vis spectrophotometer (Thermo Scientific)
- Electrophoresis power supply (PowerPac basic power supply; Bio-Rad, cat. no. 1645050)
- Mini Trans-Blot cell (Bio-rad, cat. no. 1703811)
- Mini-Protein TGX gels (Bio-rad, cat. no.456-1094)
- Mini Trans-Blot filter paper (Bio-rad, cat. no. 1703932)
- ChemiDoc XRS+ system (Bio-rad, cat. no. 1708265)
- Plant growth chamber (FH-740 Z190, HiPoint, Taiwan, China)

Software

- SEQUIN (written by Ned Seeman)
- CanDo (https://cando-dna-origami.org)
- NanoScope Analysis v1.50 (http://nanoscaleworld.bruker-axs.com/nanoscaleworld/forums/t/812.aspx)
- GraphPad Prism 7.0a (https://www.graphpad.com/scientific-software/prism/)
- Fiji ImageJ 2.0.0 (https://imagej.net/Fiji/Downloads)

Reagent setup

10× TM buffer

To make 100 ml of 10× TM buffer, mix 2.42 g of Tris base, 10.16 g of $MgCl_2 \cdot 6H_2O$ and 90 ml of Milli-Q water. Use HCl to adjust the solution to pH 8.0, and fill the solution to a final volume of 100 ml. Use a 0.22-μm filter membrane to purify the buffer. The buffer can be stored at 4 °C for up to 6 months. **! CAUTION** $MgCl_2$ is extremely hygroscopic. Buy small bottles, store in moisture-free conditions, and do not store opened bottles for long periods of time.

10× TAEM buffer

To make 1 l of 10× TAEM buffer, add 48.5 g of Tris base, 26.8 g of $MgAc_2 \cdot 4H_2O$ and 7.5 g of EDTA-2Na to 800 ml of Milli-Q water, and mix to dissolve. Use CH_3COOH to adjust the pH of the solution to 8.0, then add Milli-Q water to a final volume of 1 l. Use a 0.22-μm filter membrane to purify the buffer. The buffer can be stored at 4 °C for up to 6 months.

1× TAEM buffer (40 mM Tris base, 20 mM CH_3COOH, 2 mM EDTA and 12.5 mM magnesium acetate, pH 8.0)

Add 100 ml of 10× TAEM buffer to 900 ml of Milli-Q water and mix the solution. The buffer can be stored at 4 °C for up to 6 months.

1× PBS buffer

Add 100 ml of 10× PBS (Corning) to 900 ml of Milli-Q water and mix the solution. The buffer can be stored at 4 °C for up to 6 months.

10% (wt/vol) APS

Add 5 g of APS to 50 ml of Milli-Q water, and mix to dissolve. The solution can be stored at 4 °C for up to 3 months.

10× transfer buffer

To make 1 l of 10× transfer buffer, add 30.3 g of Tris base, 144 g of glycine to 800 ml of Milli-Q water, and mix to dissolve. Then add Milli-Q water to a final volume of 1 l. The buffer should be stored at 4 °C for up to 6 months.

1× transfer buffer

To make 1 L of 1× transfer buffer, add 100 ml 10× transfer buffer, 200 ml methanol to 700 ml Milli-Q water and mix the solution. The buffer needs to be stored at 4 °C, and it is better to prepare the buffer before running each experiment.

10× Tris-buffered saline buffer (1 M Tris, 1.5 M NaCl, pH 7.4)

To make 250 ml of 10× Tris-buffered saline (TBS) buffer, add 30.3 g of Tris base, 21.9 g of NaCl to 200 ml of Milli-Q water and mix to dissolve. Use HCl to adjust the pH of the solution to 7.4, then add Milli-Q water to a final volume of 250 ml. The solution can be stored at 4 °C for up to 6 months.

1× TBST buffer

Add 50 ml of 10× TBS buffer and 500 μl of Tween 20 (0.1% (vol/vol)) to 500 ml Milli-Q water and mix the solution. The buffer can be stored at 4 °C for at least 1 month.

Lysis buffer (10 mM Tris/HCl, 150 mM NaCl, 1 mM EDTA, 0.1% (vol/vol) NP-40, 5% (vol/vol) glycerol and 1% (vol/vol) protease inhibitor cocktail, pH 7.5)

To make 100 ml of lysis buffer, add 1.21 g of Tris base, 0.877 g of NaCl, 29.24 mg of EDTA, 0.1 g of NP-40 and 5 ml of glycerol to 80 ml of nuclease-free water, mix to dissolve, adjust the pH to 7.5 by HCL, add 1 ml of protease inhibitor cocktail, and fill the final volume to 100 ml using nuclease-free water. The buffer can be stored at −20 °C for at least 6 months.

Equipment setup

All equipment listed in the 'Equipment' section should be set up, run and maintained according to manufacturers' instructions.

Procedure

Preparation and concentration calculation of DNA/RNA stock solutions ● Timing ~1 h

1 Order DNA/RNA sequences according to Supplementary Table 1 (for non-modified DNA sequences, use standard desalting purification; for RNA and modified DNA, such as Cy3 and biotin, order with HPLC purification). Once you receive the DNA package, centrifuge the tubes at 16,000*g* at RT for 5 min to concentrate lyophilized DNA product at the bottom of the tube.

! CAUTION Do not open the tube lid before centrifugation, otherwise the lyophilized DNA powder can escape the tube and cause loss of the DNA product.

2 Dissolve DNA samples in nuclease-free water: add a certain volume of water to each sample to generate 100 μM DNA stocks, where the volume added will vary according to the molar mass and yield of DNA ordered. Dilute 2 μl of stock DNA solutions with 198 μl of nuclease-free water for UV–Vis spectroscopy measurements to confirm the DNA concentration.

▲ CRITICAL STEP Make sure the DNA is completely dissolved before dilution, by tapping the tube several times and then spinning down the solution.

3 Calculate the concentration (c) of stock DNA solutions by using the Beer–Lambert law: $A = \varepsilon bc$ (A is the absorbance, no units; b is the path length of the sample, usually expressed in cm; ε is the extinction coefficient provided by IDT), and dilute each sample to 50 μM with nuclease-free water.

▲ CRITICAL STEP It is important to precisely measure and aliquot concentrations of all DNA/RNA strands, since their stoichiometric ratios are critical for the precise assembly of DNA nanostructures.

4 Divide each sample into 10-μl aliquots, label each tube, and store at −20 °C for downstream use.

▲ CRITICAL STEP Dividing the samples into aliquots is to protect the DNA from repeated freeze–thaw cycles.

■ PAUSE POINT DNA stock solutions can be stored at −20 °C for at least 1 year.

Preparation of DNA nanostructures

5 Mix the appropriate DNA strands at a proper molar ratio in a certain volume in 1× TM or 1× TAEM buffer to form the corresponding nanostructure. Use option A for the tetrahedron nanostructure. Use option B for DHT monomers or nanostring nanostructures.

(A) **Preparation of DNA tetrahedrons ● Timing 30 min**

(i) Prepare the following mixture, where strand A, B, C and D correspond to the four single-stranded DNA oligonucleotides (see details in Supplementary Table 1) that assemble into a tetrahedron structure in 1× TM buffer:

Component	Volume	Final concentration
A (50 μM)	2 μl	1 μM
B (50 μM)	2 μl	1 μM
C (50 μM)	2 μl	1 μM
D (50 μM)	2 μl	1 μM
10× TM buffer	10 μl	1× TM buffer
Milli-Q water	82 μl	
Total volume	100 μl	

To create different sized tetrahedron nanostructures, use the corresponding DNA strands listed in Supplementary Table 1. To create the Cy3-labeled tetrahedron, replace A strand with Cy3-A. To create a tetrahedron with a 15-nt overhang for siRNA attachment, replace A strand with A-15 (see detailed sequences in Supplementary Table 1).

(ii) Heat the mixture at 95 °C for 10 min, and next cool it to 4 °C within 30 s in a PCR thermal cycler to form the tetrahedron nanostructures.

■ PAUSE POINT DNA nanostructures can be stored at 4 °C for 1 month.

(B) **Preparation of DHT monomers and nanostring** ● **Timing 24 h**

(i) Prepare the following mixtures for monomers A and B, respectively:

Monomer A

Component	Volume	Final concentration
H1 (50 μM)	2 μl	1 μM
H2 (50 μM)	2 μl	1 μM
H3 (50 μM)	2 μl	1 μM
H4 (50 μM)	2 μl	1 μM
10× TAEM buffer	10 μl	1× TAEM buffer
Milli-Q water	82 μl	
Total volume	100 μl	

Monomer B

Component	Volume	Final concentration
H5 (50 μM)	2 μl	1 μM
H6 (50 μM)	2 μl	1 μM
H7 (50 μM)	2 μl	1 μM
H8 (50 μM)	2 μl	1 μM
10× TAEM buffer	10 μl	1× TAEM buffer
Milli-Q water	82 μl	
Total volume	100 μl	

(ii) To form the DHT monomers, seal the mixed solution in a tube and put the tube in an insulated water bath (preheated to 95 °C), turning off the water bath, and letting the water bath and sample cool down from 95 °C to RT over 20 h. To synthesize the DHT monomer A with a 15-nt overhang at the center, replace H1 strand with H1-15, and to synthesize the DHT monomer A with a 15-nt overhang at the side, replace H2 strand with H2-15. To generate the biotin-labeled DHT monomer, replace the H1 strand with Bio-H1, and to make the Cy3-labeled DHT monomer, replace the H1 strand with Cy3-H1. See detailed sequences in Supplementary Table 1.

(iii) To form the nanostring, incubate the mixture (as shown in the below table) of monomer A, monomer B and initiator at 25 °C for 1 h. To generate the nanostring with a 15-nt overhang, use monomer A with overhangs at the center instead. To generate the biotin-labeled nanostring, use biotin-labeled monomer A instead, and to generate the Cy3-labeled nanostring, use a Cy3-labeled monomer A for the nanostructure assembly.

Nanostring

Component	Volume	Final concentration
Monomer A (1 μM)	2 μl	100 nM
Monomer B (1 μM)	2 μl	100 nM
Initiator (0.1 μM)	2 μl	10 nM
1× TAEM buffer	14 μl	
Total volume	20 μl	

▲ **CRITICAL STEP** Make sure to seal the tube with parafilm tightly when immersing the solution into the water bath to prevent evaporation.

▲ **CRITICAL STEP** Experimental applications (nanostructure internalization studies versus gene silencing studies) require different DNA nanostructure concentrations. For example, for the internalization studies, we use 400 nM nanostructure; for silencing evaluation, we

use 100 nM nanostructure. The final concentration of the DNA tetrahedron, monomers and nanostring can be adjusted by changing the quantities of DNA stock solutions used for nanostructure assembly.

■ **PAUSE POINT** DNA nanostructures can be stored at 4 °C for 1 month.

Characterization of DNA nanostructures

6 There are several options for characterizing the DNA nanostructures formed in the previous step. Use option A for PAGE characterization, option B for agarose electrophoresis characterization and option C for AFM characterization. For general users, we suggest choosing option A for tetrahedron and DHT monomers, and option B or C for nanostring (depending on access to an AFM).

(A) **Native PAGE gel characterization** ● **Timing 3 h**

(i) Prepare a 10% (wt/vol) native PAGE gel.

(ii) Add 2 ml of 30% (wt/vol) acrylamide/bis, 0.6 ml of 10× TAEM, 60 µl of 10% (wt/vol) APS and 6 µl of TEMED to 3.4 ml of Milli-Q water. Mix the tube by vortexing, and pour the mixture into the gel cassette. After the cassette is fully filled, insert the comb until the teeth are completely immersed. Allow the gel to polymerize for 15–20 min at RT.

! CAUTION Unpolymerized acrylamide, bisacrylamide, and APS are all neurovirulent. TEMED is toxic and corrosive. Wear lab coat, gloves and goggles, and work in a fume hood when handling these reagents.

▲ **CRITICAL STEP** Wash the gel cassette and the comb before casting the gel. Make sure there are no bubbles in the cassette before inserting the comb. Do not allow the gel to polymerize longer than 30 mins.

(iii) Prepare samples by adding 1 µl of 6× loading dye to 5 µl of 1 µM DNA tetrahedron or DHT monomer structures that were assembled in Step 5.

(iv) Load the DNA ladder and samples in recorded gel lanes, and perform electrophoresis at 80 V for 2 h in 1× TAEM running buffer.

(v) Stop the electrophoresis and stain the gel in a container containing 1× SYBR Gold (diluted from manufacturer stock 10,000 times) in Milli-Q water for 10–15 min.

! CAUTION SYBR Gold is a suspected mutagen and a possible carcinogen. Wear proper PPE and work in a fume hood when handling this reagent.

(vi) Image the gel using a gel image analysis system (Typhoon FLA 9500, excitation at 488 nm with a gain of 350 V) to characterize the formation of DNA nanostructures.

(vii) Compare nanostructure running lengths according to their predicted sizes referenced in Supplementary Fig. 1. More detailed information can be found in our previously published papers[23,44].

? TROUBLESHOOTING

(B) **Agarose gel electrophoresis characterization** ● **Timing 2.5 h**

(i) Prepare a 0.5% (wt/vol) agarose gel containing 1× SYBR Gold nucleic acid gel stain. Add 0.25 g of agarose and 5 µl of 10,000× SYBR Gold to 50 ml of 1× TAEM buffer. Heat the mixture in a microwave for ~1.5 min to make sure the agarose is fully dissolved, and pour the solution into the gel cassette. After filling the cassette, insert the comb until the teeth are completely immersed in the gel. Allow the gel to polymerize for ~30 min.

! CAUTION SYBR Gold is a suspected mutagen and a possible carcinogen. Wear proper PPE and work in a fume hood when handling this reagent. Do not heat the casting mixture in the microwave for too long to avoid boiling and splash out.

▲ **CRITICAL STEP** Wash the gel cassette and the comb before casting the gel. Make sure there are no bubbles in the cassette before inserting the comb.

(ii) Prepare samples by adding 1 µl of 6× loading dye to 5 µl of 0.1 µM nanostring as assembled in Step 5B(ii). Load the DNA ladder and samples in denoted lanes and perform electrophoresis in a 4 °C cold room at 80 V for at least 2 h in 1× TAEM running buffer.

(iii) Stop the electrophoresis after 2 h. Image the gel using a gel image analysis system (such as Typhoon FLA 9500) to characterize the formation of nanostructures.

(C) **AFM imaging of DNA nanostructures** ● **Timing 2 h**

(i) Prepare a freshly cleaved mica surface for sample adsorption.

(ii) Deposit 3–5 µl of 10 nM of the DNA nanostructures in 1× TAEM buffer from Step 5 onto the mica surface and leave it on the surface for 3–5 min. Rinse the surface with Milli-Q water and dry the surface with nitrogen gas gently.

▲ CRITICAL STEP It is critical to rinse the surface with water to wash off the salt in the sample, otherwise the salts can influence the image and potentially break or foul the AFM tip. Be careful not to damage the samples when gently rinsing and drying the surface.

(iii) Image the samples by AFM operated in PeakForce tapping mode under air condition using super-sharp tips (model TESP-SS, Bruker) with a spring constant of 0.35 at a scanning rate of 1 Hz. Representative results can be found in Fig. 2.

▲ CRITICAL STEP The diameter of the tip is crucial for high-resolution AFM imaging, especially for the smaller tetrahedron structure. The recommended scanning area is between 500 nm^2 and 5 μm^2.

? TROUBLESHOOTING

Internalization evaluation of Cy3-labeled DNA nanostructures ● Timing 1 d

▲ CRITICAL Nanostructure internalization evaluation is performed via infiltration into a transgenic mGFP5 *Nb* plant which constitutively expresses GFP, whereby GFP signal is used as a marker for the plant cell cytosol. As such, colocalization analysis of Cy3 fluorescence with GFP fluorescence will provide a relative measure of nanostructure internalization into the cytosol, and thus nanostructure internalization efficiency.

7 Prepare the Cy3-labeled tetrahedron, DHT monomer and nanostring as detailed in Step 5; dilute the solution to a concentration of 400 nM with PBS.

8 Put 100 µl of each nanostructure solution from Step 7 into a 1-ml needleless syringe. Introduce a tiny puncture into the *Nb* plant leaf with a pipette tip on the leaf abaxial surface. Center the syringe tip at the puncture area, and gently push the syringe plunger until all the liquid is infiltrated. Remove the excess solution gently from leaf surfaces after the infiltration with a Kimwipe (Supplementary Fig. 1). Infiltrate each DNA nanostructure into one leaf, ensuring to mark the leaf surface area into which the nanostructure was infiltrated. Use separate plants for each nanostructure, and separate leaves for each infiltration.

▲ CRITICAL STEP Make sure there are no bubbles inside the syringe when performing the infiltration. If air is infiltrated into the leaves, it may cause tissue deformation or damage. Orient the syringe outlet upright, and gently tap the syringe to remove any bubbles interspersed within the solution before infiltration.

9 Gently mark the area of infiltration with a Sharpie marker to make note of which area(s) received the nanostructure solution, so you can locate the treated tissue sample for downstream imaging, qPCR or western blot analysis. Wait 12 h for DNA nanostructures to internalize before imaging.

10 To image the tissue, cut a small (~2 cm × 2 cm) section of leaf tissue from the infiltrated area of the leaf and put the tissue on a glass slide with the abaxial leaf surface facing upward. Cover with a microscopy coverslip, and add 20–50 µL water between the slide and coverslip. Image through the abaxial side of the leaf with the appropriate filter sets. Here a Zeiss LSM 710 confocal microscope was employed to image the plant tissue with two channels: 488 nm laser excitation with a GFP filter cube (emission collection window: 490–520 nm) and 514 nm laser excitation with a Cy3 filter cube (emission collection window: 530–600 nm). The images were obtained with air immersion of the objective at 20× magnification.

▲ CRITICAL STEP Cut and handle the leaf tissue gently, and make sure there are no water bubbles or air bubbles between the leaf and coverslip. Press the tissue tightly between the slide and coverslip to remove water accumulation between the leaf and coverslip. If there is water between the coverslip and leaf tissue, fluorescence intensity will be lowered and the field of view will appear dark, so avoid imaging that area.

11 Confocal imaging data can be analyzed with ImageJ to quantify the colocalization fraction between the GFP channel and the Cy3 channel across all samples. For each biological replicate sample, collect at least 15 technical replicates (15 non-overlapping confocal fields of view from each leaf). All 15 fields of view can then be averaged to obtain a mean colocalization value (using ImageJ, Colocalization Analysis and Colocalization Threshold plugins) for that sample. It is recommended to take four biological replicates (four leaves per one plant), and average over biological replicates to generate a final colocalization value, which correlates with the colocalization fraction between the Cy3-tagged nanostructure and cytosolic GFP channels for each sample.

■ PAUSE POINT Following analysis of infiltration efficiency, DNA nanostructures can be adjusted and redesigned for increased internalization efficiency into plant cells, following the rules discussed in the experiment design section.

siRNA loading on DNA nanostructure loci and characterization ● Timing 3 h

▲ CRITICAL We can design a fully complementary 15-base-pair nucleotide overhang into each DNA nanostructure. The DNA tetrahedron has one attachment locus at one of its apexes with the 15-base-pair oligonucleotide overhang (see overhang sequence in Supplementary Table 1). A DHT monomer contains one attachment locus with the same 15 oligonucleotide overhang at either its center (DHT-c) or side (DHT-s). Multiple DHT-c monomers are assembled into one nanostring with corresponding cargo attachment loci (Fig. 3). These overhangs are used to hybridize the nanostructure with the duplexed siRNA.

12 siRNA duplex formation: to synthesize the duplex siRNA with a 15-nt overhang, mix two corresponding fully complementary RNA oligonucleotides (sense-15 and antisense strands target GFP or ROQ1 in Supplementary Table 1) in PBS buffer as noted below and heat to 95 °C for 5 min, followed by cooling to RT over 30 min.

Component	Volume	Final concentration
Sense-15 (10 μM)	5 μl	1 μM
Antisense (10 μM)	5 μl	1 μM
10× PBS	5 μl	1× PBS
Nuclease-free water	35 μl	
Total volume	50 μl	

13 Hybridization of DNA nanostructures with double-stranded siRNA: mix DNA nanostructures with overhangs with the preformed siRNA duplex in 1× PBS (see details in the following table) at 37 °C for 30 min at a final concentration of 100 nM for both the nanostructure and the siRNA duplex, allowing conjugation of siRNA to the DNA nanostructures.

Component	Volume	Final concentration
siRNA duplex with 15-nt overhang (1 μM)	10 μl	100 nM
DNA nanostructures with overhangs (1 μM)	10 μl	100 nM
1× PBS	80 μl	
Total volume	100 μl	

14 Gel characterization of siRNA-loaded DNA nanostructures. Use 10% (wt/vol) PAGE (option A) for analysis of the DNA tetrahedron and DHT monomer nanostructures. Use 0.5% (wt/vol) agarose gel electrophoresis (option B) for analysis of the nanostring structure.

(A) **10% (wt/vol) Native PAGE characterization**

(i) Prepare a 10% (wt/vol) native PAGE gel following Step 6A, load the DNA ladder and corresponding samples prepared in Step 13, then run the gel in 1× TAEM running buffer at 80 V for at least 2 h.

(ii) Stain the gel using SYBR Gold, image the gel with a gel image analysis system (Typhoon FLA 9500, excitation with 488 nm) and analyze the bands with ImageJ. Representative gel results can be found in Fig. 4a (tetrahedron) and Fig. 4b (DHT monomer).

(B) **Agarose gel electrophoresis characterization**

(i) Prepare a 0.5% (wt/vol) agarose gel according to Step 6B.

(ii) Prepare samples by adding 1 μl of 6× loading dye to 5 μl of 1 μM siRNA-loaded nanostring as assembled in Step 13. Load the DNA ladder and samples in denoted lanes, and perform electrophoresis in a 4 °C cold room at 80 V for at least 2 h in 1× TAEM running buffer.

(iii) Stop the electrophoresis after 2 h. Image the gel using a gel image analysis system to confirm an upward band shift for loading of the siRNA duplex onto the DNA nanostructures. Representative gel results can be found in Fig. 4c.

■ PAUSE POINT The siRNA-loaded DNA nanostructures can be stored at 4 °C for 2–3 d.

? TROUBLESHOOTING

Gene silencing evaluation

15 Infiltrate the siRNA-loaded DNA nanostructures following Steps 7–9, and evaluate the gene silencing efficiency of siRNA-loaded DNA nanostructures with three orthogonal methods:

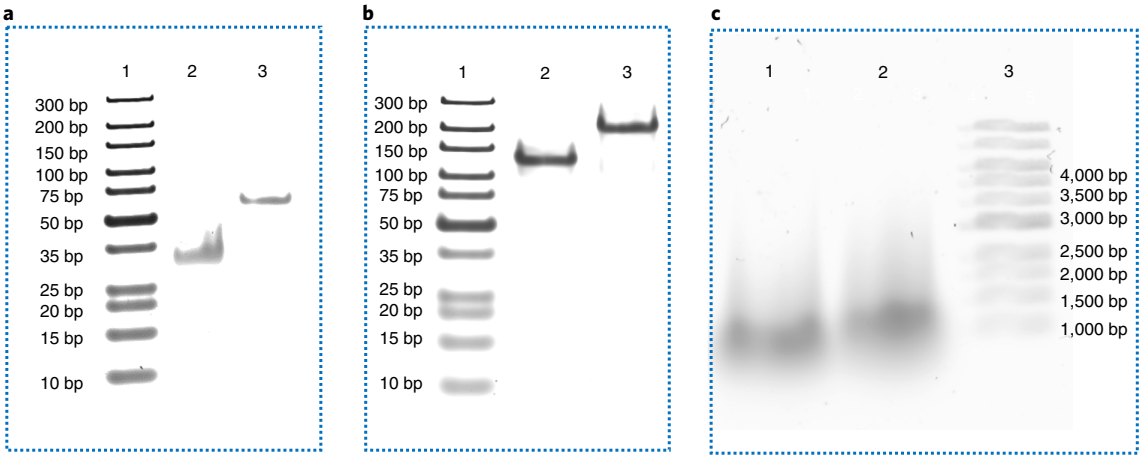

Fig. 4 | Representative gel image for characterization of the siRNA loading on DNA nanostructures. a, PAGE gel lane 1: marker; lane 2: tetrahedron with 15-nt overhang; lane 3: siRNA-loaded tetrahedron complex. **b**, PAGE gel lane 1: marker; lane 2: DHT monomer with 15-nt overhang at the center; lane 3: siRNA-loaded DHT monomer complex. **c**, 1% (wt/vol) Agarose gel lane 1: nanostring with 15-nt overhang; lane 2: siRNA-loaded nanostring complex; lane 3: marker.

(A) qPCR (mRNA level change); (B) confocal microscopy (GFP protein intensity change); (C) western blot (GFP protein amount change). Negative controls should be included: infiltrating nanostructures without siRNA should show no change in GFP mRNA expression. We recommend to check gene silencing with at least two of these methods, using option A for mRNA change and option B or C for protein change depending on the target gene of interest.

(A) **qPCR** ● **Timing 5 h**

(i) At 24 h after infiltration of each sample, cut the infiltrated leaf area (maximum of 100 mg leaf tissue) and extract the total RNA with an RNeasy plant mini kit. Remember, immediately grind the tissue in liquid nitrogen with a mortar and pestle after cutting the leaf to make sure gene expression levels do not change.

! CAUTION Handle liquid nitrogen carefully. Protect hands and eyes with Cryo gloves and safety goggles, always wear appropriate PPE (lab coat, closed-toed shoes and long pants).

(ii) Following the RNA extraction protocol, measure the concentration of the total extracted RNA using a NanoDrop spectrometer, and reverse-transcribe 1 μg of total RNA into cDNA using an iScript cDNA synthesis kit.

▲ CRITICAL STEP Make sure there is no DNA or protein contamination (the ratio of A_{260} to A_{280} should be 1.8–2.1) while extracting the total RNA. It is recommended to use DNase to digest any possible DNA contamination following RNA extraction. Sterilize your hands and working environment to protect RNA from degradation.

■ PAUSE POINT cDNA can be stored at 4 °C or −20 °C overnight.

? TROUBLESHOOTING

(iii) Use PowerUp SYBR green master mix (Applied Biosystems) for the qPCR step with 2 μl of cDNA from the previous step, and with primers designed (see detailed sequences in Supplementary Table 1) for the target gene (GFP) and a reference or housekeeping gene (for *Nb*, we suggest to use EF1).

▲ CRITICAL STEP It is necessary to run a reference gene (such as EF1 here) to normalize differences between plant/leaf conditions and slightly different amounts of total extracted mRNA. We recommend checking the literature for appropriate housekeeping genes, because they may differ across plant species.

(iv) Run the qPCR and analyze the data to quantify the mRNA level change using the ddCt method[51]. Obtain the normalized GFP gene expression-fold change with respect to the EF1 gene and control sample.

? TROUBLESHOOTING

(B) **Confocal microscopy** ● **Timing 20–30 min per sample**

(i) Wait 3 d post infiltration of siRNA-loaded DNA nanostructures to allow for silencing at the protein level to occur.

(ii) Cut a small (~2 cm × 2 cm) area of the infiltrated leaf tissue and put the cut tissue on a glass slide with the abaxial leaf surface facing upward. Cover with coverslip, and add 20–50 µL water between the slide and coverslip. Image through the abaxial side of the leaf with the appropriate filter sets. Here, a Zeiss LSM 710 confocal microscope was employed to image the plant tissue and collect all the GFP fluorescence intensity by *Z*-stack scanning with 488 nm laser excitation by a GFP filter cube (emission collecting window: 490–520 nm).

(iii) Analyze the data (GFP fluorescence intensity) using ImageJ software.

(C) **Western blot** ● **Timing 24 h**

(i) Harvest plant leaves 3 d post infiltration with siRNA-loaded DNA nanostructures and grind them in liquid nitrogen to recover dry frozen powder.

(ii) Transfer the frozen powder to a tube with prechilled lysis buffer containing 10 mM Tris/HCl (pH 7.5), 150 mM NaCl, 1 mM EDTA, 0.1% (vol/vol) NP-40, 5% (vol/vol) glycerol and 1% (vol/vol) protease inhibitor cocktail.

▲ **CRITICAL STEP** Immerse the tube in liquid nitrogen before use, and always put the tube and buffer on ice to protect proteins. Volumes of lysis buffer must be determined in relation to the amount of tissue present. Here, for 50–100 mg tissue, we recommend 300–400 µl lysis buffer. Samples can be stored at −80 °C for later use, or kept on ice for immediate homogenization.

(iii) Lyse tissue on ice for 1–2 h, then centrifuge the tubes at 15,000*g* at 4 °C for 20 min. Following centrifugation, gently transfer the supernatants containing whole proteins to a new clean tube. Quantify total extracted proteins with a Pierce 660 nm protein assay (Thermo Fisher).

▲ **CRITICAL STEP** The protein extract should not be too dilute to avoid loss of protein. Dilute as needed for loading into the gel wells. The minimum recommended protein concentration is 0.1 mg/ml, and the optimal protein concentration is 1–5 mg/ml.

(iv) Mix the samples with a loading buffer (Laemmli Sample Buffer, containing 1% (vol/vol) of 2-mercaptoethanol) appropriate for gel electrophoresis, and boil the mixture at 95–100 °C for 5 min. Load 0.5 µg of normalized total proteins from each sample and analyze with SDS–PAGE gel (Bio-Rad precast tris/glycine gel, 4–20% gradient); run at 120 V for 60 min.

▲ **CRITICAL STEP** The amount of loaded proteins can vary and may need optimization according to the target proteins. The sample should be mixed by vortexing before and after the heating step to obtain the best resolution.

(v) Transfer the gel to a PVDF membrane in cold transfer buffer and run at 400 mA in 1× transfer buffer with methanol for no more than 60 min in a cold room with an ice block.

▲ **CRITICAL STEP** Rinse the gel 1–2 times using transfer buffer before performing the transfer, to wash off any residual SDS from running the gel. Activate the PVDF membrane in methanol for a few minutes. Perform the assembly in prechilled running buffer, and do not touch surface of the membrane. With a pencil, mark the membrane corner for the following staining step. Do not run the transfer longer than 1 h to avoid running out of protein.

(vi) Block the membrane for 1 h using 7.5% (wt/vol) BSA in 1× TBST buffer followed by overnight incubation at 4 °C with the primary GFP antibody as required (1:2,000 dilution). After washing with 1× TBST buffer three times (5 min each time), the corresponding protein bands can be probed with a goat anti-rabbit horseradish peroxidase-conjugated antibody (1:5,000 dilution; Abcam, cat. no. ab205718) for 30 min. After washing, the band can be developed by incubation with chemiluminescence (Amersham ECL prime kit) in <2 min and imaged with a ChemiDoc XRS+ system.

▲ **CRITICAL STEP** The primary GFP antibody can be reused in these 4 °C overnight conditions. You can also incubate the membrane with the primary antibody at RT for 1 h to save time without further reuse of the antibody. The dilution ratio of the primary and secondary antibody needs to be optimized depending on the protein. Do not incubate with the detection kit for more than 2 min.

(vii) Quantify the intensity of GFP bands with ImageJ software.

? TROUBLESHOOTING

Troubleshooting

Troubleshooting advice can be found in Table 2.

Table 2 | Troubleshooting table

Step	Problem	Possible reason	Solution
6A(vii)	Free DNA single strands and low yield of DNA nanostructures	The strands used for the formation of the nanostructure are not in equimolar ratios	Quantify the DNA strand concentration using the UV spectrophotometer more precisely (*A* value is between 0.1 to 0.8), measure three times and use the average value to calculate the concentration
6C(iii)	Too many deposited nanostructures that are not clearly distinguished from each other; too few nanostructures observed in AFM	The sample concentration is too high or too low; adsorption time of sample on mica is too long or too short	Increase or decrease the sample concentration accordingly, a final nanostructure concentration of 5–10 nM is recommended; increase or decrease the adsorption time for sample preparation, 3–5 min is recommended
	AFM image background is dirty	Salt in the buffer deposits and dries on the mica surface; AFM tip is dirty	Rinse the mica surface after nanostructure adsorption using Milli-Q water more times, and gently dry the surface; double check the tip, replace with new tip
14	Nanostructure not fully loaded with siRNA duplex, several bands observed in the gel	The concentration of siRNA and DNA nanostructures is not at the equal stoichiometry	Make sure to calculate the concentration of both RNA and DNA precisely, double check the formation of the siRNA duplex and DNA nanostructures separately before attempting their hybridization
		siRNA duplex is not formed well or partial degradation of RNA	Remeasure the concentration of the two RNA strand, and keep the single-strand RNA at −20 °C or −80 °C.
15A(ii)	Not enough total RNA extracted, RNA degradation, RNA contamination with DNA	Unhealthy leaf tissue, contamination during the extraction, genomic DNA in the extraction	Use healthy leaf tissue for maximal RNA extraction. Infiltrate larger volume of the sample, or do multiple leaf infiltrations at one time. Keep a sterile work environment during the extraction process. Treat extracted RNA with DNAse following RNA extraction
15A(iv)	No read or substantial variation in the quantification cycle (C_q) read copy number for the GFP gene during qPCR analysis	Missing primers or incorrect primer design	Review the primer design and qPCR process. Be careful when mixing the qPCR solutions and make sure every component is added in correct amounts. Perform multiple replicates of each sample. Check the reference gene readout to make sure the process is performed correctly
15C(vii)	No protein band is observed after the blotting	Gel is running too long, and proteins are running out of the gel	Check the molecular weight of the target protein, use a colored protein marker that can be seen by eye
		Blot membrane quality is poor, blotting process is unsuccessful	Remember to activate the membrane before doing the blot; make sure there are no bubbles between the gel and the membrane; double check the detection kit, and the imaging system setup
		Antibody cannot probe the protein	Double check the target protein detection range and specificity with the manufacturer, double check your target protein sequence to ensure the antibody can bind the target protein
	The gel band overflows, or a nonspecific band is observed	Too much protein was loaded; the probing antibody was loaded in excess, or the incubation time was too long; incubation with the detection kit solution was performed for too long	Always quantify the protein before loading; optimize the dilution ratio of antibodies; limit the incubation time with the detection kit to <2 min. Wash the membrane at least three times for 5 min each wash following incubation with antibodies

Timing

Steps 1–4, DNA strand stock solution preparation: 1 h
Step 5A, DNA tetrahedron nanostructure construction: 30 min
Step 5B, HT monomer and nanostring nanostructure assembly: 24 h
Step 6, characterization of DNA nanostructures: 6 h
Steps 7–11, internalization study of Cy3-labeled DNA nanostructures: 20–30 min per sample + overnight
Steps 12–14, siRNA loading on the specific loci of the DNA nanostructures and characterization: 4 h
Step 15A, qPCR analysis: 5 h

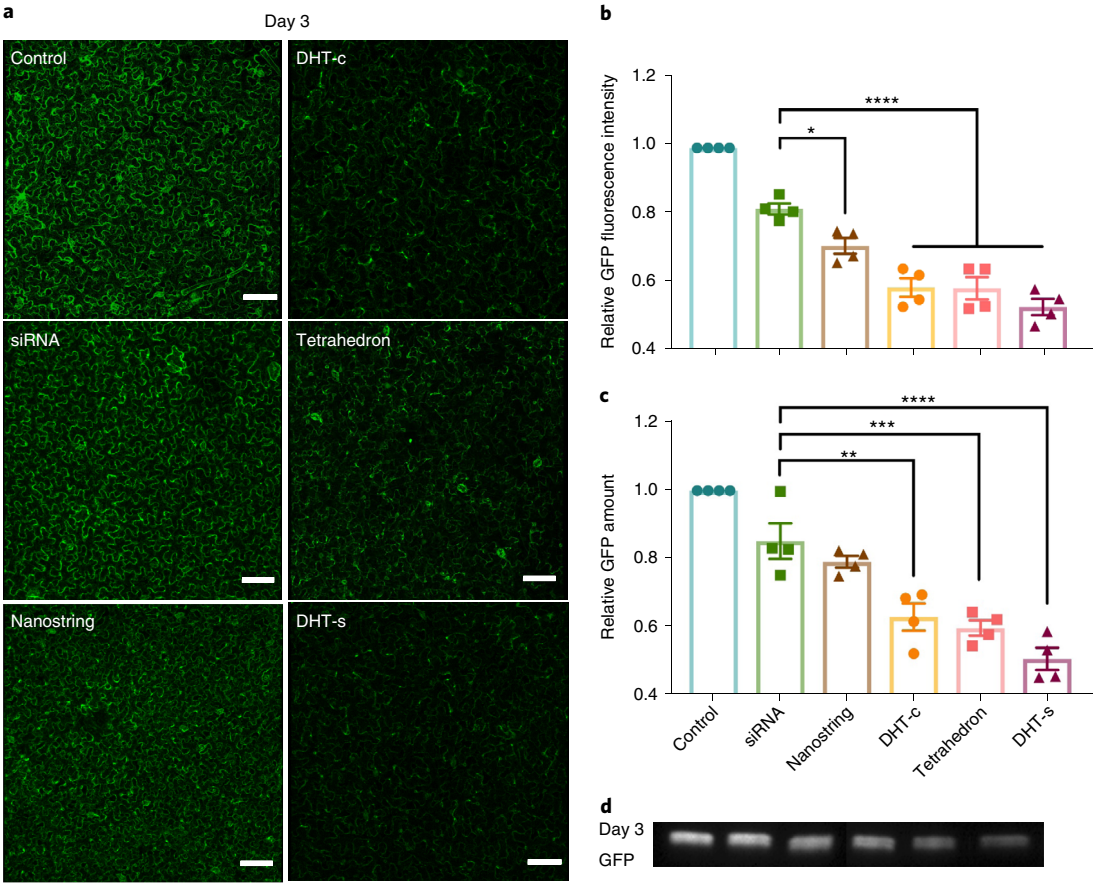

Fig. 5 | Evaluation of gene silencing efficiency 3 d post infiltration of mGFP5 *Nb* with siRNA-loaded DNA nanostructures. a, Representative confocal images showing decreased GFP fluorescence intensity following treatment with siRNA-loaded DNA nanostructures. Untreated leaves and leaves treated with free siRNA alone are used as negative controls. Scale bars, 100 μm. **b**, Quantitative fluorescence intensity analysis of confocal images. $^{*}P = 0.0151$ and $^{****}P < 0.0001$ in one-way ANOVA. Error is SEM ($n = 4$). **c**, Statistical analysis of GFP extracted from nanostructure treated leaves 72 h post-infiltration. $^{**}P = 0.0013$, $^{***}P = 0.0003$, and $^{****}P < 0.0001$ in one-way ANOVA. Error is SEM ($n = 4$). **d**, Representative western blot gel image of extracted GFP proteins 72 h post infiltration with siRNA-loaded DNA nanostructures. Adapted from ref. [25].

Steps 15B, confocal microscopy imaging: 20–30 min per sample
Steps 15C, western blot analysis of protein: 8 h + overnight

Anticipated results

Using this protocol, we anticipate that researchers will be able to construct and characterize DNA nanostructures that can act as carriers to deliver siRNA into mature plant cells to silence target genes. We have demonstrated and validated silencing in transgenic mGFP *Nb* plants with both confocal microscopy imaging (Fig. 5a,b) and western blot with qPCR analysis (Fig. 5c,d) at 3 (confocal and western blot) and 1 (qPCR) d post-infiltration. In our published results[25], we show how the above protocol can be implemented to validate that the gene silencing is transient and disappears by 7-d post-infiltration with confocal imaging, western blot and qPCR (Supplementary Fig. 6). Furthermore, we have also found that DNA nanostructure mechanical parameters, such as the size, shape, stiffness and aspect ratio can greatly influence their internalization efficiency into intact plant cells. Specifically, for the nanostructures mentioned herein, the relative internalization efficiencies are ranked as follows, from highest to lowest: DHT, tetrahedron, nanostring. The same trends are observed for protein-level silencing, with the DHT-s-loaded nanostructure silencing the most, and the nanostring-loaded nanostructure silencing the least (Fig. 5). These observations suggest that DNA nanostructures with at least one dimension smaller than 10 nm and with higher stiffness/compactness will internalize into plant cells most efficiently. Regarding mRNA-level silencing, our prior results suggest that the attachment locus between the siRNA and the nanostructure will dictate whether protein-level

silencing is accomplished via transcriptional or post-transcriptional gene silencing. Specifically, siRNA delivered to mGFP5 *Nb* via attachment to the apex of the tetrahedron nanostructure shows a strong decrease in the GFP mRNA as measured by qPCR, suggesting that the silencing mechanism is through the canonical degradation of transcriptional mRNA. However, siRNA delivered via attachment to either locus of the DHT or the nanostring shows an increase in GFP mRNA, suggesting that the silencing mechanism is through translational repression but not mRNA degradation (Supplementary Fig. 7). Because all nanostructures show protein-level silencing, we propose that the attachment locus may affect the endogenous gene silencing mechanism undertaken by the plant, as a function of the siRNA steric accessibility: siRNA is more accessible when on the vertex of the tetrahedron, and less accessible when attached to the surface of DHTs or nanostrings. Researchers should therefore consider the steric accessibility of the siRNA based on its attachment point to the DNA nanostructure if a specific gene silencing mechanism is desired. Furthermore, we show that DNA nanostructures do not induce upregulation of plant biotic and abiotic stress genes as measured with qPCR (Supplementary Figs. 8 and 9), and that we can also target silencing of an endogenous gene (ROQ1) that confers resistance against many pathogens[52,53] (Supplementary Fig. 10). We also tested the stability and likely intracellular fate of DNA nanostructures by incubating the same quantity of DNA nanostructures we employed for RNA delivery (0.01 nmol) with plant cell lysate for a range of times (0–96 h). Results in Supplementary Fig. 11 indicate that DHT nanostructures are stable for ~24 h and then are gradually degraded over time.

Reporting Summary

Further information on research design is available in the Nature Research Reporting Summary linked to this article.

Data availability

All materials are available from commercial sources or can be derived using methods described in this study. All data and controls relevant to the protocol have been included in the Supplementary Information. Raw data such as unprocessed image files can be obtained from the corresponding author upon reasonable request.

References

1. Napoli, C., Lemieux, C. & Jorgensen, R. Introduction of a chimeric chalcone synthase gene into petunia results in reversible co-suppression of homologous genes in trans. *Plant Cell* **2**, 279–289 (1990).
2. Davis, M. E. et al. Evidence of RNAi in humans from systemically administered siRNA via targeted nanoparticles. *Nature* **464**, 1067–U1140 (2010).
3. Fire, A. et al. Potent and specific genetic interference by double-stranded RNA in *Caenorhabditis elegans*. *Nature* **391**, 806–811 (1998).
4. Cunningham, F. J., Goh, N. S., Demirer, G. S., Matos, J. L. & Landry, M. P. Nanoparticle-mediated delivery towards advancing plant genetic engineering. *Trends Biotechnol.* **36**, 882–897 (2018).
5. Demirer, G. S. & Landry, M. P. Delivering genes to plants. *Chem. Eng. Prog.* **113**, 40–45 (2017).
6. Pereira, A. *Plant Reverse Genetics: Methods and Protocols* (Humana Press, 2011).
7. Zhang, J. et al. Vacuum and co-cultivation agroinfiltration of (germinated) seeds results in tobacco rattle virus (TRV) mediated whole-plant virus-induced gene silencing (VIGS) in wheat and maize. *Front. Plant Sci.* **8**, 393 (2017).
8. da Cunha, N. B. et al. The next generation of antimicrobial peptides (AMPs) as molecular therapeutic tools for the treatment of diseases with social and economic impacts. *Drug Discov. Today* **22**, 234–248 (2017).
9. Xu, P., Zhang, Y. J., Kang, L., Roossinck, M. J. & Mysore, K. S. Computational estimation and experimental verification of off-target silencing during posttranscriptional gene silencing in plants. *Plant Physiol.* **142**, 429–440 (2006).
10. Kodama, H. & Komamine, A. *RNAi and Plant Gene Function Analysis: Methods and Protocols* (Springer, 2011).
11. Silva, A. T., Nguyen, A., Ye, C., Verchot, J. & Moon, J. H. Conjugated polymer nanoparticles for effective siRNA delivery to tobacco BY-2 protoplasts. *BMC Plant Biol.* **10**, 291 (2010).
12. Mitter, N. et al. Clay nanosheets for topical delivery of RNAi for sustained protection against plant viruses. *Nat. Plants* **3**, 16207 (2017).
13. Demirer, G. S. et al. Carbon nanocarriers deliver siRNA to intact plant cells for efficient gene knockdown. *Sci. Adv.* **6**, eaaz0495 (2020).
14. Sun, W. J. et al. Cocoon-like self-degradable DNA nanoclew for anticancer drug delivery. *J. Am. Chem. Soc.* **136**, 14722–14725 (2014).
15. Ruan, W. M. et al. DNA nanoclew templated spherical nucleic acids for siRNA delivery. *Chem. Commun.* **54**, 3609–3612 (2018).

16. Hu, Q. Q., Li, H., Wang, L. H., Gu, H. Z. & Fan, C. H. DNA nanotechnology-enabled drug delivery systems. *Chem. Rev.* **119**, 6459–6506 (2019).
17. Kostiainen, M. & Linko, V. DNA nanostructures as innovative vehicles for smart drug delivery. *Eur. J. Hum. Genet.* **27**, 768–769 (2019).
18. Jiang, Q., Liu, S. L., Liu, J. B., Wang, Z. G. & Ding, B. Q. Rationally designed DNA-origami nanomaterials for drug delivery in vivo. *Adv. Mater.* **31**, 1804781–1804786 (2019).
19. Sun, W. et al. Self-assembled DNA nanoclews for the efficient delivery of CRISPR–Cas9 for genome editing. *Ang. Chem. Int. Ed.* **54**, 12029–12033 (2015).
20. Madhanagopal, B. R., Zhang, S., Demirel, E., Wady, H. & Chandrasekaran, A. R. DNA nanocarriers: programmed to deliver. *Trends Biochem. Sci.* **43**, 997–1013 (2018).
21. Linko, V., Ora, A. & Kostiainen, M. A. DNA nanostructures as smart drug-delivery vehicles and molecular devices. *Trends Biotechnol.* **33**, 586–594 (2015).
22. Li, J., Fan, C., Pei, H., Shi, J. & Huang, Q. Smart drug delivery nanocarriers with self-assembled DNA nanostructures. *Adv. Mater.* **25**, 4386–4396 (2013).
23. Zhang, H. et al. Programming chain-growth copolymerization of DNA hairpin tiles for in-vitro hierarchical supramolecular organization. *Nat. Commun.* **10**, 1006 (2019).
24. Li, J. et al. Self-assembled multivalent DNA nanostructures for noninvasive intracellular delivery of immunostimulatory CpG oligonucleotides. *Acs Nano* **5**, 8783–8789 (2011).
25. Zhang, H. et al. DNA nanostructures coordinate gene silencing in mature plants. *Proc. Natl Acad. Sci. USA* **116**, 7543–7548 (2019).
26. Bastings, M. M. C. et al. Modulation of the cellular uptake of DNA origami through control over mass and shape. *Nano Lett.* **18**, 3557–3564 (2018).
27. Webster, D. E. & Thomas, M. C. Post-translational modification of plant-made foreign proteins; glycosylation and beyond. *Biotechnol. Adv.* **30**, 410–418 (2012).
28. Withers, J. & Dong, X. N. Post-translational regulation of plant immunity. *Curr. Opin. Plant Biol.* **38**, 124–132 (2017).
29. Bila, H., Kurisinkal, E. E. & Bastings, M. M. C. Engineering a stable future for DNA-origami as a biomaterial. *Biomater Sci.* **7**, 532–541 (2019).
30. Altpeter, F. et al. Advancing crop transformation in the era of genome editing. *Plant Cell* **28**, 1510–1520 (2016).
31. Wang, P., Lombi, E., Zhao, F. J. & Kopittke, P. M. Nanotechnology: a new opportunity in plant sciences. *Trends Plant Sci.* **21**, 699–712 (2016).
32. Baulcombe, D. RNA silencing in plants. *Nature* **431**, 356–363 (2004).
33. Meister, G. & Tuschl, T. Mechanisms of gene silencing by double-stranded RNA. *Nature* **431**, 343–349 (2004).
34. Johansen, L. K. & Carrington, J. C. Silencing on the spot. Induction and suppression of RNA silencing in the Agrobacterium-mediated transient expression system. *Plant Physiol.* **126**, 930–938 (2001).
35. Dalakouras, A. et al. Induction of silencing in plants by high-pressure spraying of in vitro-synthesized small RNAs. *Front. Plant Sci.* **7**, 1327 (2016).
36. Tang, W., Weidner, D. A., Hu, B. Y., Newton, R. J. & Hu, X. H. Efficient delivery of small interfering RNA to plant cells by a nanosecond pulsed laser-induced stress wave for posttranscriptional gene silencing. *Plant Sci.* **171**, 375–381 (2006).
37. Cheon, S. H. et al. Effective delivery of siRNA to transgenic rice cells for enhanced transfection using PEI-based polyplexes. *Biotechnol. Bioproc. E* **22**, 577–585 (2017).
38. Unnamalai, N., Kang, B. G. & Lee, W. S. Cationic oligopeptide-mediated delivery of dsRNA for post-transcriptional gene silencing in plant cells. *FEBS Lett.* **566**, 301–310 (2004). 307.
39. Numata, K., Ohtani, M., Yoshizumi, T., Demura, T. & Kodama, Y. Local gene silencing in plants via synthetic dsRNA and carrier peptide. *Plant Biotechnol. J.* **12**, 1027–1034 (2014).
40. Bao, W. L., Wang, J. Y., Wang, Q., O'Hare, D. & Wan, Y. L. Layered double hydroxide nanotransporter for molecule delivery to intact plant cells. *Sci. Rep.* **6**, 26738 (2016).
41. Schwartz, S. H., Hendrix, B., Hoffer, P., Sanders, R. A. & Zheng, W. Carbon dots for efficient siRNA delivery and gene silencing in plants. Preprint at https://www.biorxiv.org/content/10.1101/722595v1 (2019).
42. Winfree, E., Liu, F., Wenzler, L. A. & Seeman, N. C. Design and self-assembly of two-dimensional DNA crystals. *Nature* **394**, 539–544 (1998).
43. Dirks, R. M. & Pierce, N. A. Triggered amplification by hybridization chain reaction. *Proc. Natl Acad. Sci. USA* **101**, 15275–15278 (2004).
44. Lin, M. H. et al. Programmable engineering of a biosensing interface with tetrahedral DNA nanostructures for ultrasensitive DNA detection. *Angew. Chem. Int. Ed.* **54**, 2151–2155 (2015).
45. Nicot, N., Hausman, J. F., Hoffmann, L. & Evers, D. Housekeeping gene selection for real-time RT-PCR normalization in potato during biotic and abiotic stress. *J. Exp. Bot.* **56**, 2907–2914 (2005).
46. Kim, H. *et al.* 'Shotgun DNA synthesis' for the high-throughput construction of large DNA molecules. *Nucleic Acids Res.* **40**, e140 (2012).
47. Castro, C. E. et al. A primer to scaffolded DNA origami. *Nat. Methods* **8**, 221–229 (2011).
48. Douglas, S. M. et al. Rapid prototyping of 3D DNA-origami shapes with caDNAno. *Nucleic Acids Res.* **37**, 5001–5006 (2009).

49. Liu, Q. et al. Carbon nanotubes as molecular transporters for walled plant cells. *Nano Lett.* **9**, 1007–1010 (2009).
50. Tang, W. et al. Post-transcriptional gene silencing induced by short interfering RNAs in cultured transgenic plant cells. *Genomics Proteomics Bioinformatics* **2**, 97–108 (2004).
51. Schmittgen, T. D. & Livak, K. J. Analyzing real-time PCR data by the comparative C_T method. *Nat. Prot.* **3**, 1101–1108 (2008).
52. Thomas, N. C. *et al.* Roq1 confers resistance to *Xanthomonas*, *Pseudomonas syringae* and *Ralstonia solanacearum* in tomato. Preprint at https://www.biorxiv.org/content/10.1101/813758v2 (2020).
53. Schultink, A., Qi, T. C., Lee, A., Steinbrenner, A. D. & Staskawicz, B. Roq1 mediates recognition of the *Xanthomonas* and *Pseudomonas* effector proteins XopQ and HopQ1. *Plant J.* **92**, 787–795 (2017).
54. Chuang, C. F. & Meyerowitz, E. M. Specific and heritable genetic interference by double-stranded RNA in *Arabidopsis thaliana*. *Proc. Natl Acad. Sci. USA* **97**, 4985–4990 (2000).
55. Schweizer, P., Pokorny, J., Schulze-Lefert, P. & Dudler, R. Double-stranded RNA interferes with gene function at the single-cell level in cereals. *Plant J.* **24**, 895–903 (2000).
56. Klahre, U., Crete, P., Leuenberger, S. A., Iglesias, V. A. & Meins, F. High molecular weight RNAs and small interfering RNAs induce systemic posttranscriptional gene silencing in plants. *Proc. Natl Acad. Sci. USA* **99**, 11981–11986 (2002).
57. Kwak, S.-Y. et al. Chloroplast-selective gene delivery and expression in planta using chitosan-complexed single-walled carbon nanotube carriers. *Nat. Nanotechnol.* **14**, 447–455 (2019).
58. Demirer, G. S. et al. High aspect ratio nanomaterials enable delivery of functional genetic material without DNA integration in mature plants. *Nat. Nanotechnol.* **14**, 456–464 (2019).

Acknowledgements

Hu. Z. acknowledges the support of the Chinese National Natural Science Foundation (21605153). The authors acknowledge support from a Burroughs Wellcome Fund Career Award at the Scientific Interface (CASI), a Stanley Fahn PDF Junior Faculty Grant under award no. PF-JFA-1760, a Beckman Foundation Young Investigator Award, a USDA AFRI award, a grant from the Gordon and Betty Moore Foundation, a USDA NIFA award, a USDA-BBT EAGER award, support from the Chan-Zuckerberg Foundation and an FFAR New Innovator Award (to M.P.L.). G.S.D. is supported by a Schlumberger Foundation Faculty for the Future Fellowship. The authors also acknowledge support from UC Berkeley Molecular Imaging Center (supported by the Gordon and Betty Moore Foundation), the QB3 Shared Stem Cell Facility and the Innovative Genomics Institute (IGI).

Author contributions

Hu. Z. and M.P.L designed the experiments, and C.F. helped with the experimental design. Hu. Z. and Ho. Z. performed the simulations and experiments. Hu. Z. and G.S.D analyzed the data and created the figures. Hu. Z., Ho. Z., G.S.D, and E.G.-G. wrote the manuscript. All authors revised and approved the manuscript.

Competing interests

The authors declare no competing interests.

Additional information

Supplementary information is available for this paper at https://doi.org/10.1038/s41596-020-0370-0.

Correspondence and requests for materials should be addressed to M.P.L.

Peer review information *Nature Protocols* thanks Veikko Linko and the other, anonymous, reviewer(s) for their contribution to the peer review of this work.

Reprints and permissions information is available at www.nature.com/reprints.

Publisher's note Springer Nature remains neutral with regard to jurisdictional claims in published maps and institutional affiliations.

Received: 14 December 2019; Accepted: 29 May 2020;
Published online: 17 August 2020

Related links
Key references using this protocol
Zhang, H. et al. *Proc. Natl Acad. Sci. USA* **116**, 7543–7548 (2019): https://doi.org/10.1073/pnas.1818290116
Zhang, H. et al. *Nat. Commun.* **10**, 1006 (2019): https://doi.org/10.1038/s41467-019-09004-4

nature research

Corresponding author(s): Markita Landry

Last updated by author(s): Apr 24, 2020

Reporting Summary

Nature Research wishes to improve the reproducibility of the work that we publish. This form provides structure for consistency and transparency in reporting. For further information on Nature Research policies, see Authors & Referees and the Editorial Policy Checklist.

Statistics

For all statistical analyses, confirm that the following items are present in the figure legend, table legend, main text, or Methods section.

n/a	Confirmed
☐	☒ The exact sample size (*n*) for each experimental group/condition, given as a discrete number and unit of measurement
☐	☒ A statement on whether measurements were taken from distinct samples or whether the same sample was measured repeatedly
☐	☒ The statistical test(s) used AND whether they are one- or two-sided *Only common tests should be described solely by name; describe more complex techniques in the Methods section.*
☒	☐ A description of all covariates tested
☐	☒ A description of any assumptions or corrections, such as tests of normality and adjustment for multiple comparisons
☐	☒ A full description of the statistical parameters including central tendency (e.g. means) or other basic estimates (e.g. regression coefficient) AND variation (e.g. standard deviation) or associated estimates of uncertainty (e.g. confidence intervals)
☐	☒ For null hypothesis testing, the test statistic (e.g. *F*, *t*, *r*) with confidence intervals, effect sizes, degrees of freedom and *P* value noted *Give P values as exact values whenever suitable.*
☒	☐ For Bayesian analysis, information on the choice of priors and Markov chain Monte Carlo settings
☒	☐ For hierarchical and complex designs, identification of the appropriate level for tests and full reporting of outcomes
☐	☒ Estimates of effect sizes (e.g. Cohen's *d*, Pearson's *r*), indicating how they were calculated

Our web collection on statistics for biologists contains articles on many of the points above.

Software and code

Policy information about availability of computer code

Data collection	N/A
Data analysis	N/A

For manuscripts utilizing custom algorithms or software that are central to the research but not yet described in published literature, software must be made available to editors/reviewers. We strongly encourage code deposition in a community repository (e.g. GitHub). See the Nature Research guidelines for submitting code & software for further information.

Data

Policy information about availability of data

All manuscripts must include a data availability statement. This statement should provide the following information, where applicable:

- Accession codes, unique identifiers, or web links for publicly available datasets
- A list of figures that have associated raw data
- A description of any restrictions on data availability

The data that support this study are available within the paper and its Supplementary Information. All primary data underlying the figures reported in the article can be obtained from the corresponding author upon reasonable request.

Field-specific reporting

Please select the one below that is the best fit for your research. If you are not sure, read the appropriate sections before making your selection.

☒ Life sciences ☐ Behavioural & social sciences ☐ Ecological, evolutionary & environmental sciences

Life sciences study design

All studies must disclose on these points even when the disclosure is negative.

Sample size	No statistical measures were used to predetermine sample size. We typically performed three or four biological replicates for each experiment.
Data exclusions	None
Replication	All statistical data shown in this paper are based on the two paper we published in Nature Communications [2019, 10 (1), 1006] and PNAS [2019, 116 (15) 7543-7548]
Randomization	images all collected randomly for the internalization study and silencing evaluation
Blinding	No. For internalization study, we collect the image in two separate channels with the GFP as reference channel, of which the fluorescence is continuous and everywhere in the cell. There is no bias for the image we take and the further analysis is through image J, and the values are generated automatically by the software, with no interference by the person who did the analysis.

Reporting for specific materials, systems and methods

We require information from authors about some types of materials, experimental systems and methods used in many studies. Here, indicate whether each material, system or method listed is relevant to your study. If you are not sure if a list item applies to your research, read the appropriate section before selecting a response.

Materials & experimental systems

n/a	Involved in the study
☐	☒ Antibodies
☒	☐ Eukaryotic cell lines
☒	☐ Palaeontology
☒	☐ Animals and other organisms
☒	☐ Human research participants
☒	☐ Clinical data

Methods

n/a	Involved in the study
☒	☐ ChIP-seq
☒	☐ Flow cytometry
☒	☐ MRI-based neuroimaging

Antibodies

Antibodies used	Anti-GFP antibody - ChIP Grade (ab290), Rabbit polyclonal to GFP; Goat Anti-Rabbit IgG H&L (HRP) (ab205718)
Validation	Anti-GFP antibody - ChIP Grade (ab290) is a highly versatile antibody that gives a stronger signal than other anti-GFP antibodies available. On Western blot the antibody detects the GFP fraction from cell extracts expressing recombinant GFP fusion proteins and has also been shown to be useful on mouse sections fixed with formalin. In Immunocytochemistry, the antibody gives a very good signal on recombinant YES-GFP chimeras expressed in COS cells (McCabe et al. 1999 and figure below). It is routinely used in Immunoprecipitation (IP) and IP-Western protocols and has been used successfully in HRP Immunohistochemistry at 1:200 on whole-mount mouse embryos. This anti-GFP antibody recognizes the enhanced form of GFP as well (https://www.abcam.com/gfp-antibody-chip-grade-ab290.html#top-640). The antibody used for conjugation reacts with rabbit immunoglobulins of all classes. Cross-reactions as determined by ELISA for the unconjugated antibody (ab182016): Mouse IgG, rat IgG, and chicken IgY, less than 2%. Human IgG, less than 7% (https://www.abcam.com/goat-rabbit-igg-hl-hrp-ab205718.html).